

Response to Reviewer # 1

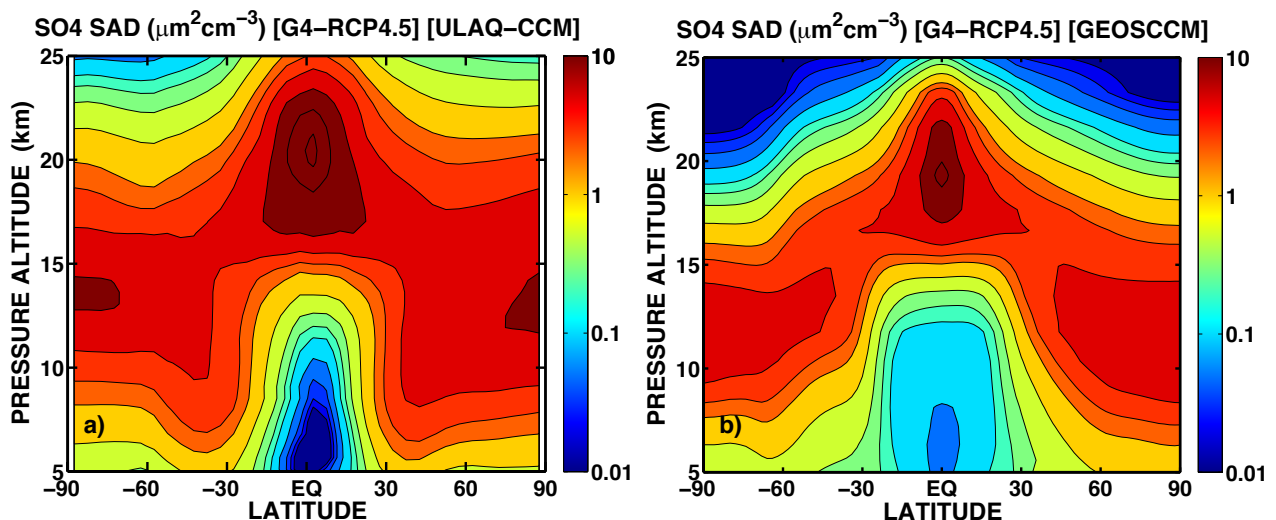
Reviewer's comments are in blue. Author responses are in black.

We thank the reviewer for his helpful comments, that will allow us to clarify some of the points of the manuscript.

My main issue is probably between minor and major. There is something that I think needs to be done but I hope can be accomplished without a great deal of difficulty (so sorry if the score looks severe).

My main concern with the paper is that they are discussing the impact of geoengineering using sulfate aerosol but never really show how their aerosol manifests itself. This is really crucial since if the aerosol is poorly depicted the rest of the results are essentially uninteresting. Is aerosol properly trapped at low latitudes above 20 km or does it run rapidly off to high latitudes (like it does in WACCM)? Looking at the aerosol SAD anomalies, I see effectively no change in aerosol loading in low latitudes. This is at odds with what was observed after Pinatubo where a normally low aerosol region in the tropical upper troposphere is filled with aerosol for several years after the eruption (mostly due to sedimentation I suspect). In any case, I think it is critical to demonstrate that their model can produce realistic aerosol distributions for this scenario. My concern is that since they apparently see no enhancement in the tropical upper stratosphere that something unrealistic is happening with the aerosol. Please make my concerns go away.

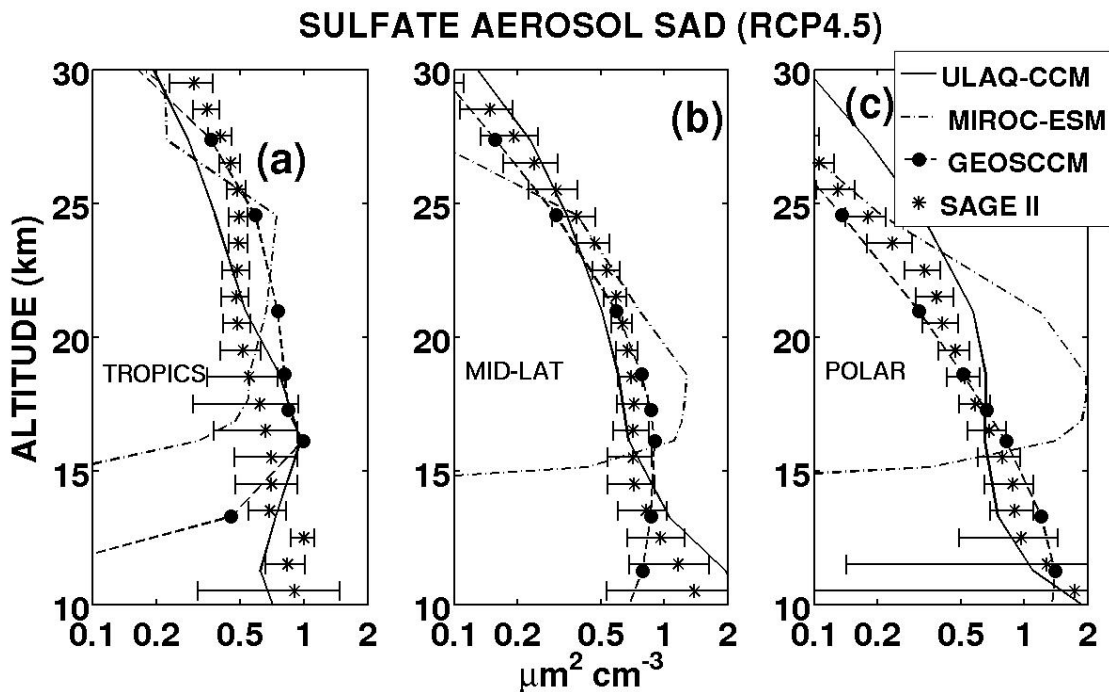
An in depth validation of both models regarding aerosol SAD changes due to SG and sulfate transport was already given in the Pitari et al. (2014) paper; we felt that adding a similar model evaluation would have lengthened the paper too much. However, in the (new) supplementary material file, we have added a new figure (Fig. S7, attached below for clarity) highlighting the aerosol SAD changes produced by SG in both models up to 25 km altitude. The original Fig. 12 (now Fig. 9 in the revised version) will remain to highlight the changes in aerosol SAD in the upper troposphere, which is closely related to the discussion in Section 5 of the manuscript (tropospheric chemistry changes).

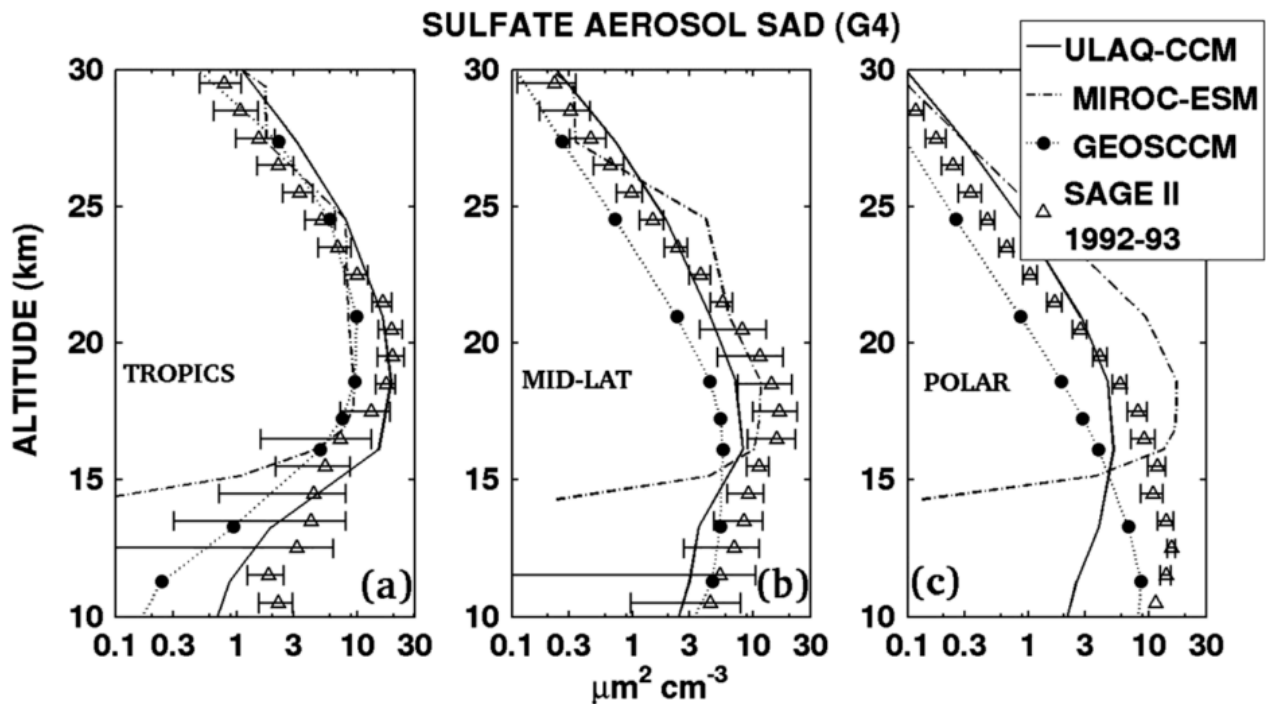


As it can be seen in the two panels, the aerosol distribution in both models reflects a good isolation the tropical pipe, in agreement with observations after the Pinatubo eruption (SAGE II, for instance) and other modeling studies (Tilmes et al., 2015). Both models show a pronounced

confinement in the tropical lower stratosphere, with an increase of both SAD and mass density in the tropical upper troposphere. The latter is produced by gravitational sedimentation of the aerosol particles and gradually approaches low values when penetrating downwards, due to irreversible removal mechanisms, namely ice particle sedimentation and wet deposition (see also Visioni et al. , 2017). A significant mid-high latitude increase of the aerosol concentration is also predicted in both models in the mid-upper troposphere, due to strat-trop exchange associated to the lower branch of the Brewer-Dobson circulation.

Differences between the two models in the aerosol distribution are due to intrinsic model differences in the size distribution (imposed for GEOSCCM and calculated for ULAQ-CCM) and the adopted radiation scheme (with impact on heating rates and hence on circulation changes). Large scale transport differences may also contribute, and the reasons are well summarized in Table 1 (treatment of QBO, SSTs, horizontal/vertical resolution). Nevertheless, both models still remain well within the range of the SAGE II measurements after the Pinatubo eruption (see Pitari et al., 2014). For good measure, we attach below a copy of Fig. 6 from Pitari et al. (2014), showing this comparison for RCP4.5 and G4 conditions (SAGE values are for 1992-1993).





Minor point, they seem to like to reference their own work an awful lot. This is ok but it left me with the impression that they are the only people doing key parts of this area of research.

We apologize if this is the impression we have given. We have tried to include all possible published works related to the topic, and if we have failed to do so we will be glad to accept any suggestion regarding an enrichment of our bibliography. Often we cite Vioni et al. (2017) because it is a review paper with a rich bibliography in this area of research, where we discussed various side effects of the sulfate injection, such as effects on ozone depletion and UV changes at the surface. However, all the relevant papers presented in that one paper are also cited here when needed, and we feel none have been left out.

Minor point, are they distributing the sulfur injection uniformly between 18 and 25 km? These seems impractical at best and more realistic injection scenarios would yield more realistic outcomes for aerosol distributions. Most scenarios I've seen suggest injection between 18 and 20 and counting on upward transport into the tropical pipe to distribute aerosol to higher altitudes (as observed following small and moderate eruptions and the well know water tape recorder).

We agree that there might be more realistic injection scenarios, but the injection scenario we used is the one prescribed by the GeoMIP G4 experiment. However, we will further expand the text in the revised manuscript about the differences in injection between the two models: the GEOSCCM model injects aerosol in the 16-25 km layer in a uniform way, the ULAQ-CCM model inject the aerosol in the 18-25 km layer, but with a Gaussian distribution that puts 80% of the sulfur mass in the altitude layer from 19.5 to 22 km. This is because the GeoMIP G4 experiment suggested to inject the aerosol in a way to mimic the way any single model handles the Pinatubo eruption (Kravitz et al., 2011).

Minor point, the uncertainties attached to SAGE II estimates of effective radius shown in the label for Table 1 are simply impossible or imply an impossible level of certainty in them. There are well known issues in estimating SAD with SAGE II observations at low aerosol levels which contributes

to significant uncertainty in a parameter derived using it (reff). At high loading, all size discrimination of optical measurements effectively go away other than 'they are big' since the spectral dependence becomes flat and invariant for large ranges of potential sizes. Certainly the authors do not shown how they were inferred and I am wondering what they mean.

We agree with the reviewer that there are large uncertainties in the SAD estimates from SAGE II, and we will add a caveat in the caption of Table 1. However, the values that we use for the effective radius (not the SAD, anyway) are the ones that have been made available by the SAGE group at the Langley Research Centre. We have changed the Table 1 caption in order to clarify that we are showing the standard deviation for the SAGE II retrieval, and not an uncertainty estimated by ourselves (see also Pitari et al., 2014).

Response to Reviewer # 2

Reviewer's comments are in blue. Author responses are in black.

This study used ULAQ-CCM and GEOSCCM to study the CH₄ transport and lifetime change under sulfate injection geoengineering. The ULAQ-CCM and GEOSCCM simulation used prescribed SSTs from CCSM-CAM4. There are only a few studies working on sulfate geoengineering impact on atmospheric chemistry, and this one is important to better understand how injected sulfate aerosol will change the stratospheric circulation and CH₄ chemistry. It is a good fit for ACP. However, more clarifications are needed.

We thank the reviewer for his in depth comments on the manuscript and for its overall positive evaluation. We have tried to address all of his comments.

More detailed model description are needed. It is not clear whether the models have land model coupled, and whether CH₄ emission is prescribed. Better explain the experiment design, such as why use two sulfate injection amounts?

We have tried to improve this part by expanding on our explanations of the models, in particular about the land-model coupling (neither GEOSCCM nor ULAQ-CCM have it), the prescribed emissions and the reason behind the different injection amounts.

There are too many figures and tables, maybe it is better to move some of them to supplemental materials, which will also make the main text more focus on its own logistic flow.

We have done what the reviewer suggested by moving Figure 2, 3 and 4, Table 4 and 5 and Figure 17 to a Supplementary Material. More figures has been added in the supplementary material, all of them mentioned in the single points raised by the reviewer below.

Specific comments:

Page 1:

-Line 3: sulfate aerosol reflects and scatters the incoming solar radiation. Reflection effect should be much larger than the scattering effect in terms of increasing the planetary albedo and cooling the surface.

Corrected.

Page 2:

-Line 3: Please change the citation format to (Kravitz et al., 2011), and change the format through the whole manuscript.

The citation format has been generated, together with the whole manuscript, with the Latex package provided by ACP, so we cannot change it. However, for other papers we have published on ACP we have found that the format is changed automatically to the one the reviewer suggested during the typesetting part of the process.

-Line 9: delete "at visible and UV wavelengths". Solar radiation is the short wave radiation.

Done.

-Line 11: change the sentence to “ a reduction of the global surface air temperature from 0.5 K (Soden et al., 2002) to 0.14 K using detrended analyses (Canty et al., 2013)”

Changed.

-Line 16: please reorganize this sentence “First of all, . . .infrared wavelengths”

We have reorganized the sentence.

-Line 27: what does “a heightened exchange between the stratosphere and the troposphere” mean? The altitude change of tropopause?

It means that the stratospheric Brewer-Dobson circulation is intensified in its advective component (i.e., the mean meridional residual circulation), so that the strat-trop exchange is larger and more CH₄ and N₂O poorer stratospheric air is advected into the troposphere.

-Line 28: change sentence to “. . .fluxes injects more stratosphere air into the troposphere, which dilute the troposphere concentration of such gases”

We have tried to rephrase the whole period so that its meaning it's clearer. The text now states *“An increase in the downward mid and high latitude fluxes in the lower stratosphere end up advecting more stratospheric air below the tropopause, thus decreasing the tropospheric concentration of these gases.”*

-Line 29: what is “the horizontal eddy mixing of UTLS tropical mixing ratios with the extra-tropics”? please reorganize.

It is the isentropic transport in the lower stratosphere, that moves in the extra-tropics those tracers with maximum concentration in the tropical pipe. The sentence has been simplified and reorganized. The text now states: *“In addition, the horizontal eddy mixing in the UTLS is lowered as a consequence of the atmospheric stabilization resulting from the tropospheric cooling and lower stratospheric warming, thus decreasing the isentropic transport of CH₄ and N₂O from the tropical pipe towards the mid latitudes. This favors an additional decrease of the UTLS extratropical downward fluxes of CH₄ and other long-lived species (Pitari et al. (2016b)).”*

Page 3:

-Line 11 - 16: move the experiment description to session 2, and add more details of the experiment design, such as what is G4? Why there are two injection amount (5/8 Tg SO₂/yr)

Done. See below for the question raised on the two injection amounts.

-Line 25-30: CCSM-CAM4 is used to provide the SST of RCP4.5 and G4 for further simulations with ULAQ-CCM and GEOCCM. Need to emphasize this. Since there are two injection amounts, maybe you should use different name for them?

CCSM-CAM4 is used only by the ULAQ-CCM model (as already stated in Table 1). We have improved Table 2 so that the amount of injection is clearer for each experiment.

Page 4:

-Line 3: what is MBC and FBC? Description needed when first appear. What's the difference among the three ULAQ-CCM experiments? How MBC and FBC make a difference?

Corrected. However, we feel that the difference among the three ULAQ-CCM experiments is clear from both Tables 1-2. MBC and FBC approaches for CH₄ make an obvious difference for the prediction of the tracer mass distribution in relation to the lifetime changes driven by OH perturbations. In the MBC approach the surface mixing ratio is assigned and fixed (it follows the time behaviour prescribed in the RCP4.5 scenario), so that the lifetime changes do not translate to a CH₄ mass distribution perturbation (except for a minimum amount in the upper troposphere). In the FBC approach (where surface CH₄ may freely respond to emission fluxes and sink processes) the tracer mass distribution responds in a coherent way to the OH-driven lifetime changes.

-Table 1: Tilmes et al. (2016) used CCSM-CAM4-CHEM, which includes stratosphere and troposphere chemistry, and performed REFC1 and REFC2 experiment. You mentioned that the G4 experiment has been done with CCSM-CAM4 without interactive chemistry. This reference might be wrong for your 8 Tg SO₂ injection case? The CCSM-CAM4 is 40 levels? In Tilmes et al. (2016), it is 26 levels (FR) or 56 levels (SD).

The reference for the CCSM-CAM4-CHEM model is correct, insofar as the same model was used as in Tilmes et al. (2016), but with no interactive chemistry (as stated). However, as the reviewer correctly noticed, the number of level is wrong. The table now states the correct number of levels, which is 26.

Why use different amount of injected SO₂ in GEOSCCM and ULAQ-CCMc relative to others?

The experiments with 5 Tg-SO₂ were the same used for Pitari et al. (2014). The ULAQ-CCM experiments with 8 Tg-SO₂ were performed in order to be consistent with G4-RCP4.5 SST changes from CCSM-CAM4, which were calculated under this larger injection hypothesis.

Table 1: in ULAQ-CCMc and GEOSCCM, RCP4.5 SSTs are used. Does the land temperature response to the sulfate injection? In that case, would there be inconsistent between the land and the ocean?

For GEOSCCM and ULAQ-CCM (c), land temperatures respond to the sulfate injection (as well to all other changes in radiatively active gases and particles), and yes, this does mean that there is an inconsistency. However, this is a common problem with AMIP style simulations. We remind the reviewer that CCMs, by definition, are atmospheric models which make climate-radiation-dynamics-chemistry (and sometimes aerosols) interact explicitly on-line, but sea surface temperatures have to be prescribed using observed data (for the past) or model predictions (for future years), based on independent predictions from AOGCMs or ESMs. In ULAQ-CCM (a) and (b) both land and sea surface temperatures are taken from CCSM-CAM4, for both RCP4.5 and G4 experiments. We agree with the reviewer that this is an important point, and Table 1 has been changed accordingly.

- general question for model description: in ULAQ-CCM and GEOSCCM, is the CH₄ emission prescribed? Or the two models have interactive land with dynamic vegetation and agriculture, CH₄ emission is interactive with the climate? Do those two models have no ocean, and that why they need the SSTs from CCSM-CAM4?

ULAQ-CCM and GEOSCCM are both, as the name suggest, CCMs. Because of this, they have no interactive ocean (as explained in the previous point), so they need SSTs from atmosphere-ocean coupled models. Just as a brief note for the reviewer: the strength of CCMs is in a highly-detailed coupling of photochemistry, radiation and climate, with a level of complexity normally higher than in coupled atmosphere-ocean models. These two CCMs, in the specific version used in the present study, are used without an explicitly interactive land-atmosphere module. Our study focuses on photo-chemically induced changes in long-lived species transport and lifetime. Future changes in land properties, potentially affecting the emission fluxes (of CH₄, in particular), are not taken in account because they are beyond our present purposes. We have tried to talk more in the model description about some model features, in order to clarify some of the points raised. However, we think that the reviewer poses an important point regarding the limitations of this study, so we have added a paragraph in the conclusion regarding the specific purpose of this study and its limitations, together with our opinion on how more complex models could further improve the analyses we have done.

We have also added, both in the model description section and in the conclusion, more references to published papers where the skills of both models where evaluated, in particular Morgenstern et al. (2017) (general up-to-date description of the models) and other related to the CCMVal-2 inter-comparison exercise.

Page 6:

-Line 2: could you explain why ULAQ-CCM has a large bias over the polar region, especially in MAR?

It is due to a combination of insufficient advective high-latitude downwelling (mean meridional residual circulation) and too strong eddy mixing, in the Southern Hemisphere high latitudes during the autumn season following the vortex break-up in November-December. This same explanation is now given in the manuscript.

-Figure 1: why TES has much higher CH₄ concentration than HALOE on both 100 hPa level and the vertical profile?

This has been explained in depth in Pitari et al. (2016a). This is what the authors had to say regarding the specific issue raised by the reviewer:

“Annually averaged zonal CH₄ mixing ratios from the FBC experiments are presented for the models, along with observations from the Aura TES thermal infrared radiances at $\lambda=8 \mu\text{m}$, corrected using co-retrieved N₂O estimates (Worden et al., 2012). The tropopause signature is well captured in the FBC model predictions, with a sudden CH₄ decrease due to downward transport of CH₄-poor stratospheric air in the downwelling branch of the extra-tropical Brewer-Dobson circulation. The tropospheric inter-hemispheric asymmetry is reasonably represented in the

models, whereas the positive vertical gradient of mixing ratios in the tropics and in the Southern Hemisphere is not replicated in model predictions. However, as discussed in Worden et al. (2012), a significant bias was found in the TES-retrieved CH₄ values in the upper troposphere with respect to the lower troposphere. A large part of this bias was adjusted by the TES team applying a correction that is based on co-retrieved N₂O estimates. After correction, a residual of 2.8% bias was still found in the upper troposphere relative to the lower troposphere.

A quantitative point-by-point spatial evaluation of the model results for the FBC case is also presented, where HALOE data (Grooss and Russel, 2005) are used for the lower stratosphere, Aura TES satellite observations for the troposphere and both datasets for the tropical upper troposphere and extra-tropical lowermost stratosphere. An average inter-hemispheric difference of 7.5% is calculated in the mid-troposphere, which is ~50% larger than the observations, which show an average of 5% inter-hemispheric difference. Tropospheric mixing ratios in the Southern Hemisphere are underestimated in the models by approximately 50 to 100 ppbv. This may be attributed to a slower horizontal eddy mixing in the tropical troposphere, with respect to real atmosphere. However, considering also the above discussed residual positive bias of the Aura/TES upper tropospheric CH₄, we may conclude that the inter-hemispheric gradient in the models is roughly consistent with observations, in their $\pm 1\sigma$ variability interval. By comparing the TES data with HALOE data, the residual bias of TES-retrieved upper tropospheric CH₄ mixing ratio is clearly visible. The models are generally within the HALOE data's 1σ uncertainty interval and thus, showing that the models have a good ability in capturing the strong horizontal gradient in the lower stratosphere, pointing out a good isolation of the tropical pipe in the models."

We feel that repeating this discussion would go beyond the scope of the present paper and lengthen it further, however we have added the reference to Pitari et al. (2016a) to that specific point of the paper.

Please use subscript number in chemical formulas, such as CH₄. Please make this change through all plots.

We feel that not using subscript numbers in the plots is graphically much better and improves readability, because it does not take up too much space. We prefer to keep the plots in this way.

-Line 12: change "significant" to "significant"

Done.

Page 7:

-Figure 2: in the figure caption, please change to "(a) and (d) 60S-90S and 60N-90N, (b) and (e) 30S-60S and 30N-60N, and (c) and (f) 30S-30N". Delete "units are ppmv". The plot itself shows the unit.

Done.

Page 9: -Table 4: instead of confidence interval, maybe standard deviation is easier to see? (e.g. ± 0.003)

The confidence interval is not plus/minus the standard deviation, as it is mentioned at page 8, line 13. We calculate the Pearson correlation coefficient r for n pairs of independent points. Since the

sampling distribution of Pearson's r is not normally distributed, the Pearson r is converted to Fisher's z-statistic and the confidence interval is computed using Fisher's z. An inverse transform is then used to return to r space. These are the step of this procedure, with rlow and rhi being our confidence interval.

Fisher Z transform:

$$z=0.5 \cdot \log\left(\frac{1+r}{1-r}\right)$$

Standard error of Z statistic:

$$stde=1.0/\sqrt{n-3}$$

low and hi values (95% confidence):

$$zlow=z-1.96 \cdot stde$$

$$zhi=z+1.96 \cdot stde$$

inverse z-transform return to r space

$$rlow=(\exp(2 \cdot zlow)-1)/\exp(2 \cdot \exp(2 \cdot zlow)+1)$$

$$rhi=(\exp(2 \cdot zhi)-1)/\exp(2 \cdot \exp(2 \cdot zhi)+1)$$

Page 10:

-Line 2: change to "model values"

Done.

-Line 8: delete "by knowing this"

Done.

-Line 10: change to "We looked at"

Done.

-Line 11: change to "Table 5 compares the coefficient. . ."

Done.

Page 11:

-Figure 4: please make sure that the title font size is the same.

Done.

Page 13:

-Line 1: would result from MBC include both the dynamic change and the tropospheric CH4 concentration change? Would it be better to put results from MBC and FBC together, and the difference will demonstrate the dynamic change?

The purpose of Figures 6 to 11 is to compare the anomalies of the two models related to changes in dynamics, to see how much they are consistent and to finally discuss the reasons of inconsistencies. To do this we can only work on MBC cases. The FBC approach is closely connected

with tropospheric chemistry issues and this is the reason why the results of ULAQ-CCM (b) are only used in the final section of the paper.

-Line 8: it might be better to change the sentence to something like “In the latter two model simulations, RCP4.5 SSTs are used, whereas ULAQ-CCM(a) is driven by G4 SSTs.”

Changed.

-Line 11: delete “where SSTs in G4 are unchanged with respect to RCP4.5.”

Removed.

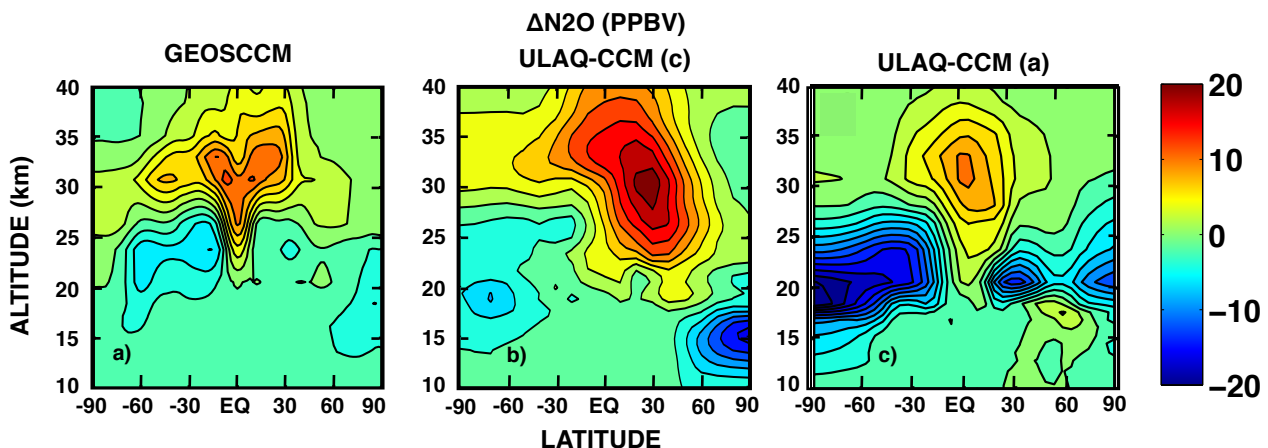
Page 14:

-Line 20: why “missing chemical processes in the upper troposphere in GEOSCCM” only affect CH₄? N₂O shows similar change in two models.

Because OH only reacts with CH₄ in the troposphere, not N₂O, thus the differences in OH do not affect N₂O and the changes are similar between models.

-Line 33: there is no zonal vertical plot showing the comparison between GEOSCCM and ULAQ-CCM (c)

We have decided not to show ULAQ-CCM (c) because in Figure 8 we are trying to discuss the differences between the simulations we decided to compare in Figure 10 and 11. However, in the supplementary material we have added a comparison between GEOSCCM, ULAQ-CCM (c), and ULAQ-CCM (a), as per the reviewer request. The figure is below.



Page 15:

-Figure 6: does the difference between GEOSCCM and ULAQ-CCM in (c) and (d) also come from the difference in QBO?

Yes, considering the similarities in the control runs (Figure 5c), the conclusion is that these differences likely come from differences in QBO. We have added this discussion in the manuscript.

-Figure 6: the difference between ULAQ-CCMa and ULAQ-CCMc in (a) and (b), is that from the gas concentration change from the troposphere or from the tropical surface temperature difference?

First of all, the difference is small. Second, it is produced by non-linear combination of the two anomalies (tropical CH₄ and N₂O concentrations and w*). But we do not think this point deserves in-depth discussion, because the anomalies are really comparable to each other. Contrary to the UTLS anomalies in the extra-tropics (SST effect) and to the much larger GEOSCCM tropical anomaly (QBO effect).

-Line 1: Why showing ULAQ-CCMa and b? do those two runs both use SSTs from G4 simulation, and ULAQ-CCMc uses SSTs of RCP4.5? if the purpose is to compare SSTs in G4 and RCP4.5, then it is a comparison between ULAQ-CCM(a),(b) and ULAQ-CCM(c).

Yes, we intended to say that we were comparing SSTs used in (a) and (b) versus the SSTs used in (c) (and the control case). We have changed this in the manuscript to make it clearer.

-Line 4: in Figure 9b, isn't the global averaged surface temperature back to RCP4.5 level around 2080? Then it is 10 years not 20 years.

There are still differences in that decade. Also by looking at the SSTs curve in Figure 9a, we can see that the differences are almost the same as the ones for the initial decade of the experiment. If we consider the "termination period" to be a phase of equilibrium similar to the control case, then two decades seem to be a better estimate than one. However, we have changed the text to say "more than one decade".

-Line 5: the warming in North Atlantic Ocean under G4 is because the cooling in that region under RCP4.5. Please look at IPCC report, and there are observations showing the cooling in that region.

We acknowledge that, in the IPCC report, there is a cooling of that particular region. And we do expect that, for the same reasons stated in the report, in case of sulfate geoengineering that region would warm. The reason for this is that an increase of sea-ice under geoengineering (because of the surface cooling) would produce saltier waters, which being denser would go deeper when moving south, allowing for warmer sea surface temperatures. So when these two effects combine, we obtain the warming we see in the anomalies that we are discussing. We have added a short explanation for what happens in the RCP4.5 scenario in the manuscript.

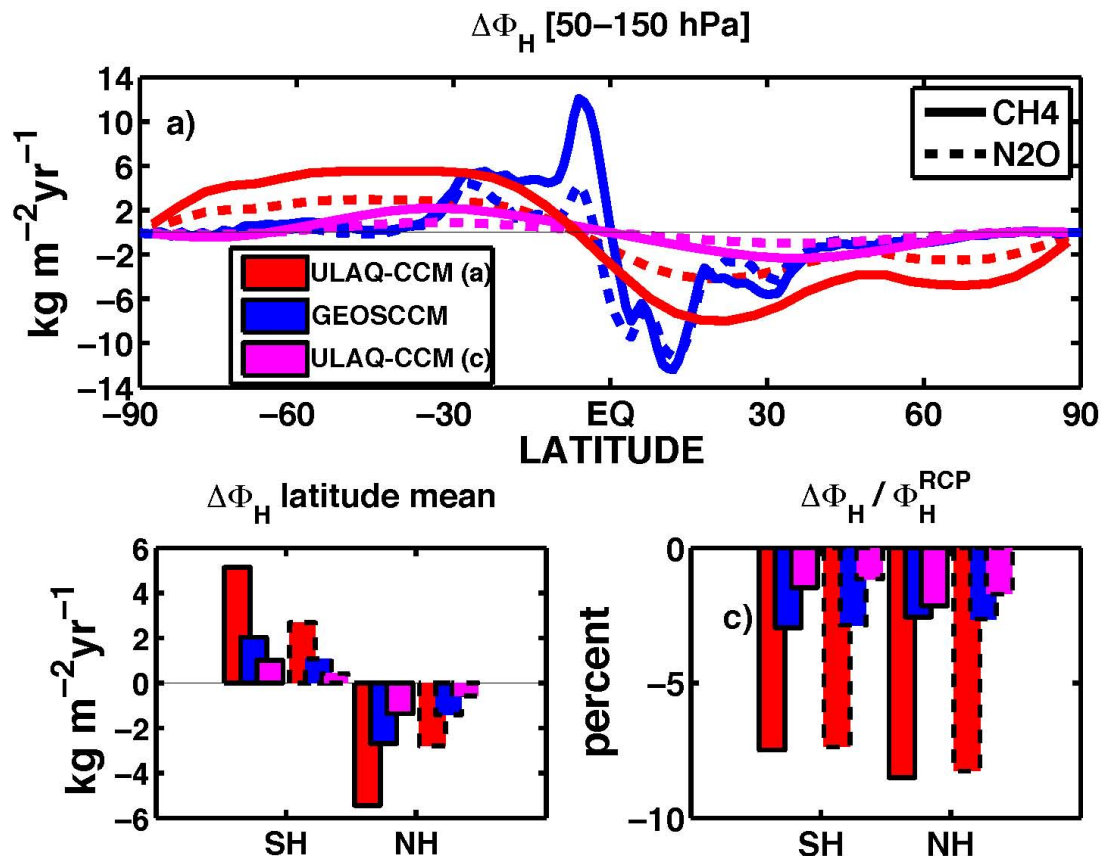
However, comparing the IPCC report to our experiment is, in a way, wrong. The IPCC report studies the time evolution of surface temperatures under a given emission scenario (for example RCP4.5) and the anomalies are time-anomalies (i.e., future years versus present time). On the other hand, in our study on the potential SG impact, the anomalies are among two different scenarios at a given time horizon, so that the fact that under RCP4.5 that region of the North Atlantic is cooling down, cannot explain why CCSM-CAM4 predicts a warming under SG. The explanation we propose (based on differences in deep water formation) may however apply to both anomalies.

Page 16:

-Line 8: why comparing ULAQ-CCMa and GEOSCCM? ULAQ-CCMa simulates 8Tg SO₂/yr injection, and used SSTs of G4, GEOSCCM simulates 5Tg SO₂/yr injection, and used SSTs of RCP4.5.

We wanted to highlight the changes due to the inclusion (or not) of varying SSTs, while also comparing differences between the two models. We have decided not to include the ULAQ-CCM

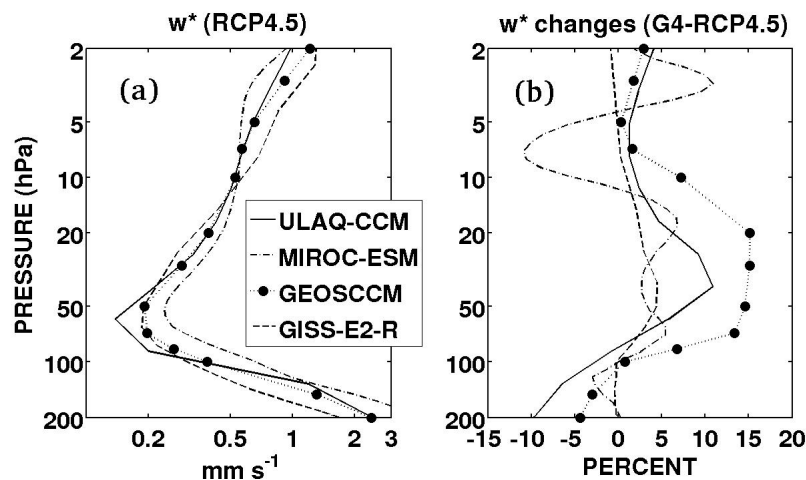
(c) results in Figures 10 and 11, because the inter-model differences were not as important in this case. The inclusion of varying SSTs produces much larger differences (mainly in the UTLS) with respect to those attributable to 8 or 5 Tg-SO₂ injection. For the sake of completeness, we have included in the Supplementary material a direct comparison of long-lived species anomalies due to changes in dynamics, for GEOSCCM, ULAQ-CCM (c) and ULAQ-CCM (a), as mentioned above. Furthermore, we have added a figure in the supplementary that is the same as Figure 11 in the manuscript, but including also the values for ULAQ-CCM (c) in it. While we still think that the comparison between GEOSCCM and ULAQ-CCM (a) is the focus of the section, we believe that adding ULAQ-CCM (c) to the supplementary material could help convince any reader that, like the reviewer, might have the same doubts. The figure is below.



We would like to answer here this reviewer request, made also ahead in his comment. Pressure altitude (that we sometime refer to as simply Altitude) is the atmospheric altitude calculated with a fixed scale height (7 km in our case), so that it is not a geometric altitude, but a way to show a log-pressure scale. Anyway it is a classical definition, with plenty of examples in the literature. We prefer to stick with pressure altitude on the y axis, which is indeed pressure: only a log operation has to be done.

-Figure 8: figure 6 shows that the vertical mass flux in GEOSCCM is much larger than in ULAQ a and c as a result of QBO, why here the stratosphere CH4 concentration is much stronger in ULAQ? Is that because the troposphere CH4 concentration is much higher in ULAQ than in GEOSCCM?

Figure 6 shows the vertical mass flux anomaly averaged from 5 to 50 hPa and from 20S to 20N. It is a mass flux anomaly, so that it is obvious that in the average the vertical layer closer to 50 hPa has a much higher relative importance with respect to the upper part. In the lower layer there are clear regions of negative tracer anomalies in the ULAQ-CCM (a) case, for the reasons widely discussed in the manuscript. In addition, it is important to remind that Fig. 6 compare fluxes, whereas Fig. 8 shows the final changes produced on the tracers distribution, which are a function of the flux divergence, with coupling of vertical and horizontal motions. The flux anomalies presented in Fig. 6 are essentially (but not exactly) a proxy of the w^* anomalies, that are larger in GEOSCCM mainly for the different treatment of the QBO (internally generated in this model). A figure from Pitari et al. (2014) is included below, which summarizes SG induced w^* anomalies among different models (including GEOSCCM and ULAQ-CCM).



-Figure 8: why there are strong reduction of CH4 and N2O under G4 in lower stratosphere over the south pole relative to RCP4.5 using ULAQ?

We have explained the reason in the discussion for Figures 9, 10 and 11. In particular, we note that the stronger reduction of both lived species in the Southern Hemisphere is caused by a more efficient perturbation in the stratospheric mean meridional circulation. The greater the increase of descent (Fig. 10), the greater the penetration of long lived species poorer air in the UTLS.

-Line 6: how was the lifetime calculated?

The atmospheric lifetime is calculated the way is supposed to, i.e., integrated tracer mass in the atmosphere divided by the integrated chemical loss of the tracer. We start from daily values of

both quantities, we divide them and finally we average the daily results over the time period considered. Taking into account that this is a textbook definition, and that there are no others, we do not feel that there is the need to add any further description in the manuscript.

Page 18:

-Figure 9: In (b) G4 global averaged surface temperature returns back to RCP4.5 level around 2080, but in (a) the red dashed line (2080-2089) shows a large negative number, with a global average close to -0.5 K. How could that be?

We think the problem might be on how the global average is considered. If the global average on Fig. 9a is performed as a weighted (by the cosine of latitude) average (as it should be done), then the number is not so close to -0.5 K, and is indeed less than 0.3 K. This is the same value visible in Fig. 9b, when the whole decade is considered.

Page 19: -Figure 10: the red and blue bars are overlapped.

Page 20: -Figure 11: the red and blue bars are overlapped.

This is a choice we made considering both readability and the presence of a finite space. We feel that our choice is correct and we would like to stick to it.

Page 21: -Line 8-9: delete the repeat sentence.

Done, thank you.

-Line 17: what does $2 \times 10 \text{ um}^2 \text{ cm}^{-3}$ mean? Should it be 2-10?

Yes, we meant the range 2 to 10. We clarified.

Page 22:

-Figure 12: what does Pressure Altitude mean? Add pressure level in y-axis.

See the reply above regarding Figure 8.

-Line 4: 10-30%

Corrected.

Page 23:

-Line 1: how about over the mid-high latitude regions, UVB increases as a net result, which enhances the production of OH.

It is meaningless to attempt a one-by-one correlation between tropospheric UVB and OH changes. We have spent a good part of the manuscript to highlight that there is an overlap of causes determining the final net OH change, in any given part of the atmosphere. In the troposphere the UVB balance is important, but very important are also the budget of H₂O (which is a function of temperature) and the budget of NO_x, which is a function of aerosol SAD and interactions with other chemical species. In addition, there are effects of O₃, CH₄ itself and so on. Taking the net

increase of mid-high latitude UVB (mainly produced by the stratospheric O₃ depletion) to find a corresponding increase in OH, is simply meaningless.

In Figure 15, does the green colour over pole regions on the surface mean positive or negative?

The green colour is the 0 level. Please consider also what is written in the point above.

-Line 3: 1.5-2.0%

Corrected.

-Line 4: unit of latitude.

Corrected.

-Line 8: not scattering increases albedo, reflection is the main reason.

Corrected. However, since the reviewer has pointed this out before, we would like to specify that reflection is nothing else but backward scattering, so every time we mentioned “scattering” we were not, per se, wrong, although surely reflection is more precise and we have changed it everywhere as suggested.

Page 27:

-Line 6: The relative long life time makes the CH₄ concentration needs a longer time to return back to the RCP4.5 level after termination. But why the lifetime of CH₄ need a long time to back to RCP4.5 level? Could you please explain more? How the atmospheric dynamics, the UVB, OH (which are related to the CH₄ lifetime) changes after the termination?

The lifetime is defined as integrated tracer mass divided by the integrated chemical sink of the tracer (both in the whole atmosphere). Now if a tracer has a lifetime of approximately 10 years and, for example, we switch off all the tracer sources at the surface, the lifetime would act as an e-folding time and we would need to wait for a time much longer of 10 years to arrive to a global atmospheric mass being for example 5% of the initial value (more or less 30 years). This view of the chemical lifetime as an e-folding time may easily convince that once a mechanism affecting the tracer production OR the tracer sink (in our case, the OH perturbation associated to SG) is suddenly stopped, then several decades are needed to go back to the unperturbed (RCP4.5) lifetime, simply because an increased atmospheric mass of the tracer has to be processed by an amount of OH close to its unperturbed RCP4.5 value. In addition, OH does not instantaneously come back to the original unperturbed value, due to many other changes that have taken place in the atmosphere (SSTs, much longer lived species as N₂O and their indirect impact on O₃, etc). But even if OH were instantaneously adjusted to the unperturbed RCP4.5 value, the tracer mass would now start its evolution from a higher value (see Fig. 15). Last, but not least, the stratospheric lifetime of CH₄ is much longer than its global ~10 years value, arriving to values even larger than 100 years (above the tropopause). Hope this clarifies.

Page 29: -Line 6: please change to “we have described that an injection of 5-8 Tg of SO₂ per year would have effect on large scale. . .”

-Line 6-8: reorganize this sentence, maybe break into two sentences.

We have used these suggestions to rephrase to sentences better.

Page 30:

-Line 1 and Figure 18: “a decrease in tropospheric UV” will be misleading. Figure 14 shows the reduction in only in tropics, and there is an increasing over mid-high latitude.

As before, we have added “tropical” because that is what drives the methane lifetime.

-Please discuss the uncertainty of this study, and what could be improved in future studies.

This has been done in the conclusion. We also modified Figure 18 so as to include the suggestion of the comment posted on ACPD by R. de Richter, and added in the conclusion all possible effects that were not included in our experiments.

Response to the Short Comment posted by R. de Richter

Comment is in blue, author response is in black.

The manuscript acp-2017-593 proposed by D. Visoni et al, is very interesting and deserves publication.

We would like to thank the writer for his comment and for taking the time to read the manuscript. We have tried to address his observations below.

Nonetheless the reader might feel that some important starting hypothesis to their study is missing and should be clearly indicated.

As a matter of fact, as it is written, the manuscript lets us make the assumption that the authors only considered the effects on the newly injected sulphates in the stratosphere by the SRM technology, without taking into consideration the current tropospheric anthropogenic emissions of SO₂ and their future evolution during the period in consideration. First, we think that, with the assumption that current anthropogenic sulphur tropospheric emissions stay stable during all the period of this study, adding extra-sulphate emissions in the stratosphere would probably increase its global deposition more evenly distributed worldwide than current tropospheric emissions. Under sulphate SRM some wetlands that previously receive low amounts or did not receive tropospheric sulphates will receive (more) sulphates, and it is known that sulphate in acid rain suppresses methane emissions from natural freshwater wetlands (Gauci et al, 2008, J. Geophys. Res.), rice paddies, peat lands and other terrestrial landscapes (Oeste and al, 2107, ESD), which are the biggest methane emitters as the authors noted in table 7 of their manuscript; thus CH₄ emissions reduction will occur.

Also, it is known that under a global warming (without sulphur SRM), warmer temperatures and increased rainfall in some regions will increase CH₄ emissions. Under the cooling SRM scenarios envisioned by the authors (first column of figure 18 of page 30), the reverse should occur.

Two new columns in figure 18 can be added as follows:

Increase in planetary albedo => surface cooling => lower temperatures => lower CH₄ emissions => lower CH₄ atmospheric concentration => shorter CH₄ lifetime

Increase in planetary albedo => surface cooling => lower rain fall => smaller wetlands area => lower CH₄ emissions => lower CH₄ atmospheric concentration => shorter CH₄ lifetime

We believe the above mentioned assumption (current anthropogenic sulphur tropospheric emissions stay stable during all the studied period) should be stated in this manuscript, as:

a) current tropospheric sulphur anthropogenic emissions are and order of magnitude larger than the ones envisioned by the authors for stratospheric SRM;

b) since China's SO₂ emissions started decreasing, the current trend is to a global decrease of tropospheric sulphur anthropogenic emissions (Klimont et al, 2013, Environ. Res. Lett.);

c) estimates of the amounts of sulphur pollution needed to reduce CH₄ emissions of the total wetland source have been made (Gauci et al, 2004, PNAS).

Second, the "clathrate gun hypothesis" has been debated by the scientific community as under a warming world, increased emissions from permafrost and/or from methane hydrates destabilisation is a risk. Recent work (Kohnert et al , 2017, Sci. Rep.) suggests that a new pathway of CH₄ emissions exist and that it may increase if ongoing permafrost thaw continues. Under the cooling SRM scenarios envisioned by the authors the reverse should occur.

One new column in figure 18 page 30 can be added as follows: Increase in planetary albedo => surface cooling => lower temperatures => lower CH₄ emissions by permafrost => lower CH₄ atmospheric concentration => shorter CH₄ lifetime.

We agree with the commenter that there are many effects that we have not considered, and considering that we used CCMs for our experiments, we felt it was clear what the limitations were. However, following his suggestion, we have added in the conclusion most of the commenter's remarks regarding other possible side-effects concerning sulfate geoengineering and CH₄. We felt, however, that changing Fig. 18 (now Fig. 14 in the revised manuscript) was not the right course of action. We have updated the title, to show what kind of effects we are referring to, and have added in the caption the ones we are not considering.

Third, we agree that the OH radical sink for CH₄ is the most important in the troposphere, but it is known that the chlorine radical sink for CH₄ is not only important in the stratosphere, but also occurs in the troposphere (Oesté and al, 2107, ESD), where it represents 3-5% of the CH₄ removal. Variations in the tropospheric acidity may change the importance of the chlorine sink for methane. With the assumption that current anthropogenic sulphur tropospheric emissions stay stable during all the period of the author's study, adding extra-sulphate emissions in the stratosphere would probably increase the tropospheric Cl content, and, as the kinetics of the reaction of Cl radical with alkanes (including methane) are an order of magnitude larger than with the OH radical, thus the chlorine radical sink for CH₄ will increase.

One new column and a new line in figure 18 page 30 can be added as follows: Increase in sulphur emissions => increased tropospheric acidity => more HCl increased Cl radical sink for CH₄ => more Cl => lower CH₄ lifetime

We believe that the authors should add in their manuscript that they made the assumption that this second CH₄ sink (the Cl radical) is assumed to stay constant in their model.

We would like to better clarify this point with the commenter: our model (ULAQ-CCM) has online an explicit and detailed chlorine-bromine photochemistry; all related species follow the prescribed time evolution by the RCP scenario in use (RCP4.5 in our case). The same also applies to GEOSCCM, by the way. In what is now Table 5, furthermore, regarding sinks and sources of methane, Cl is present as a sink and it would not be correct to state that it stays constant in time.

Response to the Short Comment posted by P.J. Nowack

Comment is in blue, author response is in black.

I think your results are also interesting in connection to air pollution under SRM - could you discuss the possible wider implications briefly in your conclusions? For context, see for example

Xia, L., Nowack, P. J., Tilmes, S., and Robock, A.: Impacts of Stratospheric Sulfate Geoengineering on Tropospheric Ozone, *Atmos. Chem. Phys. Discuss.*, <https://doi.org/10.5194/acp-2017-434>, accepted for publication. <https://www.atmos-chem-phys-discuss.net/acp-2017-434/>

Nowack, P. J., Abraham, N. L., Braesicke, P., and Pyle, J. A.: Stratospheric ozone changes under solar geoengineering: implications for UV exposure and air quality, *Atmos. Chem. Phys.*, 16, 4191-4203, <https://doi.org/10.5194/acp-16-4191-2016>, 2016.

Thank you for your comment. We think that adding some discussion on air pollution could greatly benefit our conclusions. The first paper you mentioned is already cited in regards to ozone depletion (page 22, line 9 in the discussion paper), but will also be included in the conclusions.

We have added a paragraph in the revised manuscript at the end of page 25. It states: *“In addition, gas species concentration changes (especially ozone) would also affect air quality and surface UV concentrations, which might have implications on human health, as already noted in Xia et al. (2017) and Nowack et al. (2016). As discussed in the present study, as well as in Nowack et al. (2016), Tilmes et al. (2012) and Pitari et al. (2014), the stratospheric ozone depletion induced by geoengineering solar radiation management techniques directly impact the tropospheric UV budget. The health impact of surface UV increases (located only at mid-high latitudes in the case of sulfate geoengineering) may be partly counterbalanced by the decreased tropospheric OH concentration and O₃ production.”*

Sulfate Geoengineering Impact on Methane Transport and Lifetime: Results from the Geoengineering Model Intercomparison Project (GeoMIP)

Daniele Visioni^{1,2}, Giovanni Pitari¹, Valentina Aquila³, Simone Tilmes⁴, Irene Cionni⁵, Glauco Di Genova², and Eva Mancini^{1,2}

¹Department of Physical and Chemical Sciences, Università dell'Aquila, 67100 L'Aquila, Italy

²CETEMPS, Università dell'Aquila, 67100 L'Aquila, Italy

³GESTAR/Johns Hopkins University, Department of Earth and Planetary Science, 3400 N Charles Street, Baltimore, MD 21218, USA

⁴National Center for Atmospheric Research, Boulder, CO 80305, USA

⁵ENEA, Ente per le Nuove Tecnologie, l'Energia e l'Ambiente, 00123 Roma, Italy

Correspondence to: Daniele Visioni (daniele.visioni@aquila.infn.it)

Abstract. Sulfate geoengineering ([SG](#)), made by sustained injection of SO₂ in the tropical lower stratosphere, may impact the CH₄ abundance through several photochemical mechanisms affecting tropospheric OH and hence the methane lifetime. (a) ~~Solar radiation scattering~~ [The reflection of incoming solar radiation](#) increases the planetary albedo and cools the surface, with a tropospheric H₂O decrease. (b) The tropospheric UV budget is upset by the additional aerosol scattering and stratospheric ozone changes: the net effect is meridionally not uniform, with a net decrease in the tropics, thus producing less tropospheric O(¹D). (c) The extratropical downwelling motion from the lower stratosphere tends to increase the sulfate aerosol surface area density available for heterogeneous chemical reactions in the mid-upper troposphere, thus reducing the amount of NO_x and O₃ production. (d) The tropical lower stratosphere is warmed by solar and planetary radiation absorption by the aerosols. The heating rate perturbation is highly latitude dependent, producing a stronger meridional component of the Brewer-Dobson circulation. The net effect on tropospheric OH due to the enhanced stratosphere-troposphere exchange may be positive or negative depending on the net result of different superimposed species perturbations (CH₄, NO_y, O₃, SO₄) in the extratropical upper troposphere and lower stratosphere (UTLS). In addition, the atmospheric stabilization resulting from the tropospheric cooling and lower stratospheric warming favors an additional decrease of the UTLS extratropical CH₄, by lowering the horizontal eddy mixing. Two climate-chemistry coupled models are used to explore the above radiative, chemical and dynamical mechanisms affecting CH₄ transport and lifetime (ULAQ-CCM and GEOSCCM). The CH₄ lifetime may become significantly longer (by approximately 16%) with a sustained injection of 8 Tg-SO₂/yr started in year 2020, which implies an increase of tropospheric CH₄ (200 ppbv) and a positive indirect radiative forcing of sulfate geoengineering due to CH₄ changes (+0.10 W/m² in the 2040-2049 decade and +0.15 W/m² in the 2060-2069 decade).

1 Introduction

Many geoengineering methods have been proposed in order to temporarily balance out the direct effect of the increase of anthropogenic greenhouse gases emissions (Kravitz et al. (2011)). Amongst those, stemming from the observations of the effects of large volcanic eruptions, is the injection of sulfate aerosol precursors (e.g, SO₂) into the stratosphere (Crutzen (2006), Roco et al. (2011), Kravitz et al. (2012)). The injection above the tropopause of very large amounts of particles and sulfur gases due to explosive volcanic eruptions is able to increase the stratospheric aerosol optical depth by more than one order of magnitude. The initial volcanic SO₂ plume quickly nucleates into H₂SO₄ vapor (Bluth et al. (1992)) producing an optically thick cloud of sulfate aerosols (McCormick and Veiga (1992), Lambert et al. (1993), Long and Stowe (1994)). The high reflectivity of these aerosols ~~at visible and UV wavelengths~~ effectively decreases the amount of solar radiation reaching the Earth surface, thus producing a net global cooling. In 1991, for example, the Pinatubo eruption produced a reduction ~~in of~~ the global surface air temperature ~~estimated to be a value ranging~~ from 0.5 K (Soden et al. (2002)) ~~down to~~ 0.14 K ~~globally if recent, using~~ detrended analyses (Canty et al. (2013))~~are considered~~.

Beside the direct effect on surface temperatures, however, there is the need for a thorough examination of other effects on atmospheric circulation and chemical composition of the troposphere and stratosphere brought about by the increase in lower stratosphere optical thickness (Visioni et al. (2017)). ~~First of all, connected with the increased radiation scattering by the~~ The interaction of the H₂SO₄ particles comes an increase in the ~~with solar radiation is twofold: the aerosols increase the amount of radiation that is reflected and scattered but they also absorb part of it in the near-infrared wavelengths, increasing the~~ lower stratospheric diabatic heating rates, ~~caused by the direct aerosol absorption in the near-infrared wavelengths~~. This causes a local positive temperature change (Labitzke and McCormick (1992)) which induces a significant increase of westerly winds from the thermal wind equation, with peaks at mid-latitudes in the mid-stratosphere (Pitari et al. (2016c)). These dynamical changes tend to increase the amplitude of planetary waves in the stratosphere and to enhance the tropical upwelling in the rising branch of the Brewer Dobson circulation (Pitari et al. (2014), Aquila et al. (2014)). For continuity, a stronger downward component is found in the lower branch of the Brewer-Dobson circulation (Aquila et al. (2013), Pitari et al. (2016b)).

These dynamical changes can bring about modification in the concentration and growth-rate of long-lived species that act as greenhouse gases, such as N₂O and CH₄, as observed in the case of the Pinatubo eruption (Schauffler and Daniel (1994), Dlugokencky et al. (1994)): ~~a heightened exchange between the stratosphere and the troposphere, with an~~ An increase in the downward mid and high latitude fluxes ~~would mean an injection of stratospheric air containing smaller mixing ratios of such gases in the troposphere in the lower stratosphere ends up advecting more stratospheric air below the tropopause, thus decreasing~~ the tropospheric concentration of these gases. In addition, the horizontal eddy mixing ~~of UTLS tropical mixing ratios with the extra-tropics in the UTLS~~ is lowered as a consequence of the atmospheric stabilization resulting from the tropospheric cooling and lower stratospheric warming: ~~this, thus decreasing the isentropic transport of CH₄ and N₂O from the tropical pipe towards the mid latitudes. This~~ favors an additional decrease of the UTLS extratropical downward fluxes of CH₄ and other long-lived

species (Pitari et al. (2016b)). The overall effect on tropospheric OH due this enhanced stratosphere-troposphere exchange and perturbed UTLS horizontal mixing may be positive or negative depending on the net result of different superimposed species perturbations in the UTLS (CH_4 , NO_y , O_3).

Coupled with this perturbation of the stratosphere-troposphere exchange, the lifetime of long-lived species with tropospheric OH sink can also be modified by other changes brought about by an injection of tropical stratospheric aerosols: a) the surface cooling would directly lessen the amount of water vapor, thus lowering the tropospheric OH concentration; b) the tropical tropospheric UV decrease due to enhanced radiation scattering would reduce the production of $\text{O}(^1\text{D})$, thus decreasing OH production from $\text{O}(^1\text{D}) + \text{H}_2\text{O}$; c) the increasing aerosol surface area density (SAD) would enhance heterogeneous chemistry in the mid-upper troposphere, which reduces the amount of NO_x and the rate of O_3 production, both negatively affecting the amount of tropospheric OH. Since CH_4 is depleted by the OH radical, all these changes would mean an increase in methane lifetime (Banda et al. (2013), Banda et al. (2015)). The aim of this study is to evaluate the chemical, radiative and dynamical effects of a sustained injection of SO_2 in the stratosphere on the lifetime and abundance of CH_4 .

The paper is organized in seven subsequent parts. Section 2 includes a description of participating models. In Section 3 a model evaluation for long lived species stratospheric abundance and transport is presented using available satellite observations. Section 4 analyses the sulfate geoengineering induced perturbations on stratospheric species transport, while Section 5 discusses the effects on tropospheric chemistry and CH_4 direct and indirect radiative forcing components, with the overall main conclusions discussed in Section 6.

2 Model experiments

The characteristics of the experiment follow the description of experiment G4 in the Geoengineering Model Intercomparison Project (GeoMIP) (Kravitz et al. (2011)). ~~For this experiment, the~~ The G4 experiment consists of a constant yearly injection of SO_2 in the tropical lower stratosphere. The SO_2 injection is handled by the single models in the same way they simulate the Pinatubo eruption in terms of injection height. The background anthropogenic forcing ~~profile~~ corresponds to the one from the Representative Concentration Pathway 4.5 (RCP4.5) (Taylor et al. (2012)). Starting from 2020, 8 (or 5) Tg- SO_2 /yr are injected in the stratosphere with a sudden stop after 50 years. Additional 20 years of model simulations are performed (up to 2090) in order to assess the termination effects of the sulfur injection.

~~The paper is organized in seven subsequent parts. Section 2 includes a description of participating models. In Section 3 a model evaluation for long lived species stratospheric abundance and transport is presented using available satellite observations. Section 4 analyses the sulfate geoengineering induced perturbations on stratospheric species transport, while Section 5 discusses the effects on tropospheric chemistry and CH_4 direct and indirect radiative forcing components. The choice of the different amounts of injected SO_2 follows two reasons: for some of the analyses we have decided to use the same simulations used in Pitari et al. (2014), with the overall main conclusions discussed in Section 6.~~

3 Model experiments

5 Tg-SO₂/yr. However, two experiments with varying sea surface temperatures (SSTs) have also been carried out with ULAQ-CCM to identify possible changes due to this dynamics-driving mechanisms; for this reason an injection of 8 Tg-SO₂/yr was performed with ULAQ-CCM in order to use the CCSM-CAM4 surface temperatures that resulted from a 8 Tg-SO₂/yr injection.

The main features of the participating models are summarized in Table 1.

5

One of these models (CCSM-CAM4) is an atmosphere-ocean coupled model and it has been used (without interactive chemistry) to calculate the surface temperature evolution from 2010 to 2090 for a reference RCP4.5 case and a geoengineering G4 perturbed case with 8 Tg-SO₂/yr injected continuously from 2020 to 2070 (Kravitz et al. (2011); Pitari et al. (2014)). One of the other two models (ULAQ-CCM) has assimilated ~~the sea surface temperatures (SST)~~ surface temperatures calculated in the
10 CCSM-CAM4 atmosphere-ocean coupled model for the reference RCP4.5 and the perturbed G4 cases (i.e., two different ~~SST datasets, both without interactive chemistry~~ datasets for surface temperatures), whereas the third model (GEOSCCM) has run the G4 case with RCP4.5 SSTs assimilated from the CESM atmosphere-ocean coupled model. Both models prescribe CH₄ mixing ratios at the surface (except in one numerical experiment of ULAQ-CCM where emission fluxes are used, as discussed below), and do not include changes in emission fluxes due to surface temperature modifications. A more detailed description
15 of these numerical models can be found in Tilmes et al. (2016) and Pitari et al. (2014).

In order to properly assess the different contributions to CH₄ changes discussed before, three different experiments have been carried out with the ULAQ-CCM model: experiments (a,b) use appropriate ~~SSTs~~ surface temperatures for RCP4.5 and G4 cases (as previously explained), with ~~MBC and FBC~~ surface CH₄ treated under MBC (Mixing ratio Boundary Condition) and FBC (Flux Boundary Condition) approaches for (a) and (b), respectively. Experiment (c), on the other hand, uses the same SST for both RCP4.5 and G4 cases (as in GEOSCCM), with the purpose of highlighting the impact of SST changes on the G4-RCP4.5 large scale transport perturbations. The full list of numerical experiments completed with the three models is presented in Table 2.

Table 1. Summary of main model features. Column 6 includes the stratospheric aerosol effective radius (r_{eff} in μm) at 20 km over the tropics (2040-2049). Values deduced from SAGE-II observations are: $0.22 \pm \mu\text{m}$ ($\sigma = 0.02 \mu\text{m}$) as an average over 1999-2000 for unperturbed background conditions and $0.57 \pm \mu\text{m}$ ($\sigma = 0.03 \mu\text{m}$) as an average over July 1992-June 1993 for a volcanic perturbation (i.e., Pinatubo) comparable in magnitude to G4 with 5 Tg-SO₂-Tg-SO₂ injection (in terms of average stratospheric mass burden of sulfate). G4 aerosols are injected at the equator between 16 km and 25 km altitude (uniformly) for GEOSCCM and between 18 and 25 km (gaussian distribution) for ULAQ-CCM. ~~MBC~~ → Mixing-ratio Boundary Condition. ~~FBC~~ → Flux Boundary Condition.

Model	Resolution ¹	Ocean/Land	QBO	CH ₄ Surface Boundary Condition	Stratospheric Aerosol Source
CCSM-CAM4	$1.9^\circ \times 2.5^\circ$, L40-L26 Top : 3 hPa	Coupled	No	MBC	From SO ₂ oxidation ² G4 → 8 Tg-SO ₂ [Tilmes et al. (2016)] ³
GEOSCCM	$2^\circ \times 2.5^\circ$, L72 Top : 0.01hPa	Prescribed SSTs CESM4 [CESM4, G4=RCP4.5] G4=RCP4.5 -Calculated Land Temperatures	Internal ^{3,4}	MBC	From SO ₂ oxidation ² G4 → 5 Tg-SO ₂ G4 → $r_{eff} = 0.60 \mu\text{m}$
ULAQ-CCM (a)	$5^\circ \times 6^\circ$, L126 Top : 0.04hPa	<u>Prescribed Surface</u> Prescribed SSTs - <u>Temperatures</u> [CCSM-CAM4]	Nudged	MBC	From SO ₂ oxidation ^{4,5} G4 → 8 Tg-SO ₂ G4 → $r_{eff} = 0.78 \mu\text{m}$
ULAQ-CCM (b)	As above	As above	As above	FBC	As above
ULAQ-CCM (c)	As above	Prescribed SSTs CCSM-CAM4 [CCSM-CAM4, G4=RCP4.5] G4=RCP4.5 -Calculated Land Temperatures	As above	MBC	From SO ₂ oxidation ^{4,5} G4 → 5 Tg-SO ₂ G4 → $r_{eff} = 0.61 \mu\text{m}$

¹ Latitude by longitude horizontal resolution, number of vertical layers, and model top atmospheric pressure.

² Forced with background aerosols from SAGE-II data for 1999.

³ The model is the same as described in Tilmes et al. (2016), but in this case it was run with no interactive chemistry.

⁴ QBO internally generated using a gravity wave drag parameterization and resolved wave forcing.

⁵ ULAQ-CCM includes aerosol microphysics (RCP4.5 $r_{eff} = 0.19 \mu\text{m}$)

Table 2. Summary of numerical experiments. ~~Ensemble~~, with ensemble size. The amount of injected SO₂ (per year) is specified between brackets in the G4 column.

Model	RCP4.5	G4	Used for
CCSM-CAM4	2	2 (8 Tg-SO ₂)	SSTs for the ULAQ-CCM simulation
GEOSCCM	3	3 (5 Tg-SO ₂)	Assessing CH ₄ changes due to transport
ULAQ-CCM (a)	2	2 (8 Tg-SO ₂)	Assessing CH ₄ changes due to transport
ULAQ-CCM (b)	2	2 + 1 ¹ + 1 ² + 1 ³ + (8 Tg-SO ₂)	Assessing CH ₄ changes due to chemistry
ULAQ-CCM (c)	2	2 (5 Tg-SO ₂) + 1 ⁴ (8 Tg-SO ₂)	Assessing CH ₄ changes due to transport and chemistry

¹ FBC sensitivity case [sn1] with temperature and winds from RCP4.5 in the chemistry module and continuity equations of chemical tracers.

² FBC sensitivity case [sn2] with temperature from RCP4.5 in the chemistry module.

³ FBC sensitivity case [sn3] with winds from RCP4.5 in the continuity equations of chemical tracers.

⁴ MBC sensitivity case for experiment (c), using the same sulfur injection as in experiments (a,b).

The ULAQ-CCM sensitivity cases run with the FBC approach will help in assessing the role of temperature and wind changes in the CH₄ lifetime perturbation under geoengineering conditions.

3 Model evaluation

Both ULAQ-CCM and GEOSCCM have already been extensively reviewed in the past, both on their general features (Morgenstern et al. (2010)) or for issues related to this study, such as the extratropical UTLS (Hegglin et al. (2010)), or surface UV (Bais et al. (2011)). The shortwave radiative transfer module of the ULAQ-CCM was carefully evaluated in the AeroCom intercomparison exercise of Randles et al. (2013).

In order to properly evaluate the models, regarding the specific points of this paper however, further evaluations have been done with different sets of observations have been employed (Table 3). A list of these is available in Table 3. CH₄ measurements are taken by the Halogen Occultation Experiment (HALOE), which is on board of the Upper Atmosphere Research Satellite (UARS), launched in 1991 (Russell et al. (1993)). Climatologies are formed for the period 1991-2005, based on extended datas from Grooss and Russell III (2005). HALOE measurements range from 15 to 60-130 km altitude (depending on the species) and cover 80°S to 80°N in latitude within one year. In all intercomparisons the HALOE climatological mean and the interannual standard deviation (1σ) are shown. CH₄ and N₂O profiles are estimated by Aura TES thermal infrared radiances at $\lambda=8\ \mu\text{m}$ with version 5 retrieval algorithm, where CH₄ is corrected using co-retrieved N₂O estimates (Worden et al. (2012)). Climatological mean and inter annual standard deviation for both species are calculated for the period 2004-2010. Climatological mean and inter annual standard deviation of N₂O between 2001-2005 are based on Odin/SMR product (Urban et al. (2009)). A further discussion regarding TES and HALOE differences can be found in Pitari et al. (2016a), together with a more in depth evaluation of ULAQ-CCM CH₄ predictions.

Table 3. Summary of CH₄ and N₂O satellite observations used in this study.

Observation	CH ₄	N ₂ O
TES	2004-2010	2004-2010
HALOE	1991-2005	
SMR		2001-2005

CH₄ diagnostics largely reflect the skill of the transport representation in the models. We examined climatological zonal profiles at selected latitudes, months, and pressure levels, for both model outputs and observations (Fig. 1). The climatologies refer to the years 1990-2010, in order to include the range of HALOE and TES observations. Both ULAQ-CCM and GEOSCCM compare well with observations and are normally in the $\pm 1\sigma$ deviation interval, relative to the climatological zonal mean. Some spread between models appears, more evidently in the polar regions at 100 hPa. This might be due to a combination of insufficient advective high-latitude downwelling and too strong eddy mixing in the Southern Hemisphere during the autumn season in ULAQ-CCM. GEOSCCM values are generally closer to observations than those of ULAQ-CCM. Otherwise, models perform quite similarly, and overall these diagnostics do not reveal ~~weakness~~ major weaknesses in the simulations.

A more in-depth evaluation of transport properties in the models can be found in the supplementary material regarding the correlation between CH₄ and N₂O and the mean Age of Air. The correlation between CH₄ and N₂O can be used to investigate transport properties relative to model and observations (SPARC-CCMVal (2010)). Fig. ~~?? S1~~ and Fig. ~~?? S2~~ show CH₄ vs. N₂O correlations between 100 hPa and 1 hPa ~~for models climatological mean in the same time range of TES (Fig. ??) and in the same time range of HALOE relative to CH₄ and SMR relative to N₂O (Fig. ??). In Table ??a and Table ??b. In Table S1~~ we present Pearson correlation coefficients relative to the different latitude bands ~~in both cases. Confidence interval is calculated using the Fisher transform inverse. The existence of mixing barriers at the edge of the tropical pipe allows the distinction between tropical (Fig. ??e, ??f, ??e, ??f) and midlatitude correlations (Fig. ??b, ??e, ??b ??f).~~ All these panels show a compact correlation and a good agreement with the observations; the relative Pearson coefficients in Table ~~??a and Table ??b are always significant~~ S1a and Table S1b are always significant. Panels regarding polar regions (Fig. ~~??a, ??d~~ S1a, S1d and Fig. ~~??a, ??d~~ S2a, S2d) present a larger spread with slightly lower (but still significant) Pearson coefficient between 90S-60S. In the lower stratosphere at tropical and mid latitudes there is a strong compact relationship between CH₄ and N₂O related to the slope equilibrium (Sankey and Shepherd (2003)): the mixing happens at faster time scale than the chemical loss and transport to the surface. At polar latitudes the correlation is affected by vortex edge, which represents a mixing barrier during the winter-spring season. ~~In polar regions, models display a correlation more compact compared with observed data: this happens because the latter are affected by a large uncertainty due to either: sparse coverage of the satellites data, as shown by Grooss and Russell III (2005) for HALOE or the low sensitivity of the retrieval method as shown by Worden et al. (2012) for TES. Overall values in Table ??a present a better correlation with respect to values in Table ??b: this might be a consequence of a different range of years used for CH₄ (1991-2005) and N₂O (2001-2005).~~

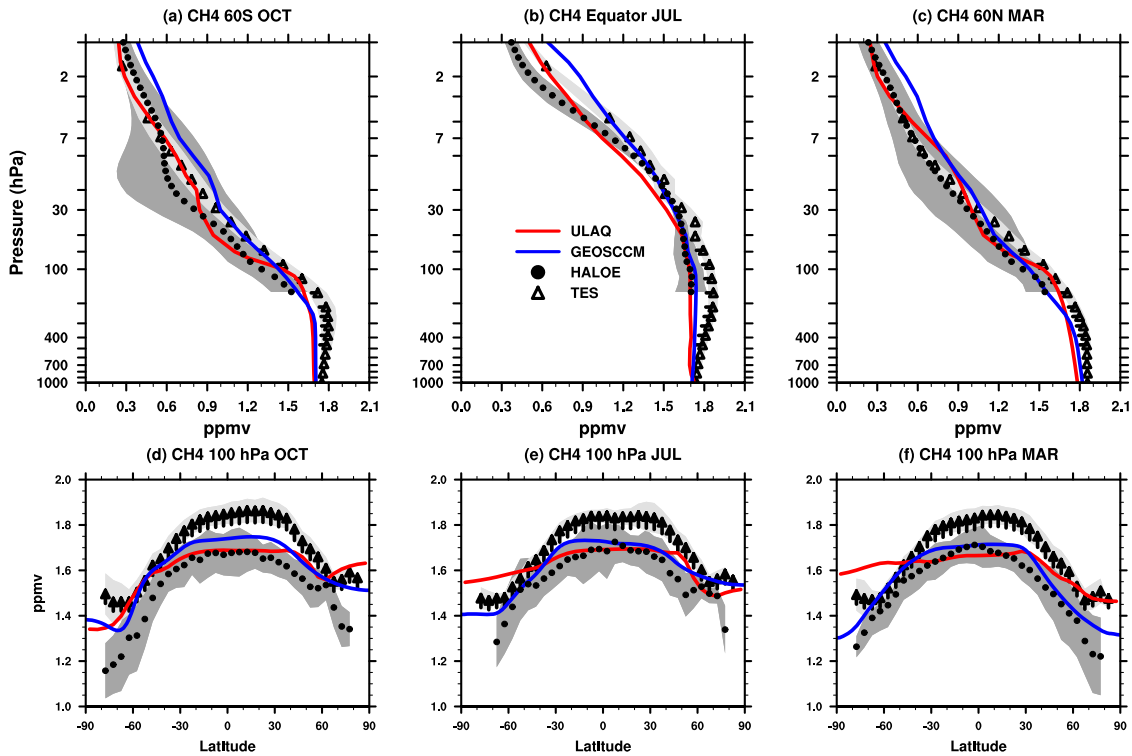


Figure 1. Evaluation of zonal and annual mean CH_4 mixing ratios ULAQ-CCM (red) and GEOSCCM (blue) simulations averaged over 1991-2010. Observations are taken from HALOE (black dots, average 1991-2005) (Grooss and Russell III (2005)) and TES Aura (black triangles, average 2004-2010).

Scatter plots of zonal and monthly mean mixing ratio values of CH_4 and N_2O for ULAQ-CCM (red) and GEOSCCM (blue) simulations, in the layer 1-100 hPa and averaged over 2004-2010. The panels refer to latitude bands 60S-90S and 60N-90N (a), 30S-60S and 30N-60N (b), 30S-30N (c). Units are ppmv. Model values are evaluated with CH_4 and N_2O data from TES observations (black), averaged over 2004-2010.

As in Fig. ??, but using observed data from HALOE for CH_4 (average 1991-2005) and SMR-Odin for N_2O (average 2001-2005) (Urban et al. (2009)). Model data are averaged over 1991-2005 for CH_4 and 2001-2005 for N_2O .

a) Pearson correlation coefficient with associated confidence interval calculated using the Fischer transform inverse, for observations and model data presented in Fig. 2 (2004-2010). b) as in a) but for the data presented in Fig. 3 (1991-2005 for the models and HALOE, 2001-2005 for SMR). (Fig. S3).

R_{Pearson} 90S-60S 60S-30S 30S-30N 30N-60N 60N-90N 0.921-0.988 0.971-0.995 0.956-0.990 0.908-0.933 0.986-0.990 0.967-0.974 0.994-0.992 0.990 0.997 0.994 GEOSCCM 0.980-0.984 0.990-0.992 0.989-0.990 0.997-0.997 0.994-0.995 0.990-0.996 0.995-0.997 0.993 ULAQ-CCM 0.988-0.991 0.995-0.996 0.994-0.995 0.997-0.998 0.992-0.994 0.761-0.958 0.952-0.970 0.926 HALOE/SMR

0.723-0.7940.951-0.9630.947-0.9570.966-0.9950.914-0.9380.978-0.990-0.990-0.996-0.995-GEOSCCM-0.976-0.9800.989-0.9910.989-0.995-0.993-0.996-0.992-ULAQ-CCM-0.979-0.9850.994-0.9950.992-0.9930.995-0.9970.991-0.993

Another important diagnostic for the evaluation of the model transport is based on the mean age of air (AoA). In particular, [the latitudinal](#) gradient between tropics and midlatitudes can be used to assess tropical ~~ascend~~[ascent](#) independently of quasi-horizontal mixing (SPARC-CCMVal (2010)). ~~Fig. ??a and Fig. ??b show tropical and midlatitudes (35N-50N) profiles of mean AoA and Figure ??c displays vertical gradients of mean AoA between 45N and the equator. The mean AoA observations are based on Andrews et al. (2001) and Engel et al. (2009) data, as presented by Strahan et al. (2011). Models profiles are very similar and in good agreement with observations.~~ Following Strahan et al. (2011), tropical mean AoA profiles (~~Fig. ??a~~) combine the effect of ascent rate and horizontal mixing. The agreement of model and observations only shows that the combined effects of ascent and mixing produce a realistic mean AoA in the models. Fig. ~~??e~~[S3c](#) identifies how ascent contribute to the overall tropical transport~~seen in Fig. ??a.~~

The horizontal gradient of mean age (~~Figure ??e~~) is able to reveal some characteristics of the Brewer-Dobson circulation (BDC) (Neu and Plumb (1999)), namely the ascent rate. In fact, differences between midlatitude and tropical values exclude horizontal mixing, since that affects equally both the tropics and midlatitudes. In GEOSCCM and ULAQ-CCM the horizontal gradient is smaller than observations up to 21 Km, indicating a fast ascent, but still included in the range of observed variability. The analysis of the relationship between mean AoA and N₂O (Fig. ~~??d~~)[validates S3d](#) [evaluates](#) the lower stratospheric transport and our use of the well-measured N₂O in Fig. ~~??S1~~ and Fig. ~~??~~. ~~The models S2. The model~~ values of mean AoA and N₂O shown represent the climatological mean (~~1980-2010~~[1980-2005](#)) in the range 10-100 hPa and 10S-10N, while observed value of mean age of air are the same as in Fig. ~~??a~~[S3a](#) and observed values of N₂O are [the](#) SMR/Odin climatological mean (2001-2005). The correlation for N₂O>150 ppbv looks compact, the slope of the model curves is similar to the observed curve; ~~models-model~~ values of N₂O and mean AoA are in the same range as the observations. Fig. ~~??e~~[S3e](#) presents the evaluation of latitudinal sections of N₂O at 50 hPa against SMR/Odin data. For tropical values, GEOSCCM and ULAQ-CCM agree very well with the observations, overall model values fall inside the 2 σ interannual variability. At northern midlatitudes ULAQ-CCM overestimates SMR; in the Southern Hemisphere GEOSCCM values are larger than SMR and ULAQ-CCM values lower.

In order to properly asses the temperature of the polar stratosphere and its interannual variability, the models must correctly simulate the vertical propagation of planetary waves from the troposphere to the stratosphere. ~~By knowing this, we can validate the models transport skill by looking at the correlation between polar temperature and~~ [Since it is possible to use the correlation between winter polar temperatures and eddy heat fluxes in the lower stratosphere as](#) a proxy for planetary wave propagation. ~~This can be done by looking~~, [we looked](#) at the correlation between the meridional heat flux at 100 hPa (40° to 80° for the two hemispheres) and the 50 hPa [polar temperatures](#) (60° to 90° for the two hemispheres)~~polar temperatures (Eyring et al. (2006)). This is shown in Table ??, where we compare the coefficient~~, [following Eyring et al. \(2006\). Table S2 in the supplementary material compares the coefficients](#) of the linear fit between the two quantities for ULAQ-CCM, GEOSCCM and the ERA40 reanalysis. The positive slope is found in both models and reanalysis, with a greater similarity in the Northern Hemisphere

with respect to the Southern Hemisphere: this difference was already shown in Eyring et al. (2006).

Vertical profiles of (a) equatorial and (b) mid-latitude AoA for GEOSCCM (blue line) and ULAQ-CCM (red line), compared with the range of observations from Andrews et al. (2001) and Engel et al. (2009) (yellow-filled area). The time average is from 1980 to 2000; the latitudinal average is 10S-10N in (a) and 35N-50N in (b). The latitudinal gradient of AoA is shown in panel (c), calculated as the difference between the Northern Hemisphere mid-latitudes and the equator (symbols and colors are as in panels (a,b)). Panel (d): scatter plot of AoA (years) versus the N₂O mixing ratio (ppmv), for GEOSCCM (blue circles), ULAQ-CCM (red circles) and the median of AoA observations from Andrews et al. (2001) and Engel et al. (2009) versus N₂O SMR observations (black circles). The time average is between 2001-2005. Panel (e): 50 hPa latitudinal section of the N₂O mixing ratio (ppbv) from the same models and observations as in panel (d). The yellow-filled area show the range of time variability of SMR measurements (i.e., $\pm 2\sigma$).

Parameters of the linear fit of polar temperatures versus eddy heat fluxes (Austin et al. (2003)). The four columns show the correlation between the heat flux at 100 hPa averaged over 40°N to 80°N for January and February versus temperatures at 50 hPa averaged over 60°N to 90°N for February and March in the Northern Hemisphere, while for the Southern Hemisphere the heat fluxes at 100 hPa are averaged between 40°S and 80°S in July and August and the temperatures at 50 hPa are averaged between 60°S and 90°S in August and September. The four columns represent, for the years 1981-2002 datas, respectively the correlation coefficient (R), the parameters for the linear fit (T_0 and β) and the related error for β . Northern Hemisphere R T_0 β σ ERA40 0.69 193.8 1.44 0.27 GEOSCCM 0.80 193.5 1.65 0.22 ULAQ-CCM 0.65 192.8 1.29 0.15 Southern Hemisphere R T_0 β σ ERA40 0.83 188.7 1.04 0.17 GEOSCCM 0.81 179.3 2.05 0.32 ULAQ-CCM 0.93 185.4 1.76 0.29

In Fig. 2 ~~ab~~ the vertical mass fluxes are evaluated by looking at the CH₄ and N₂O measurements ~~already used in Fig. ?? and Fig. ?? but this time~~ combined with the vertical velocities measured by MERRA, defining the flux as $[\rho w^*]$. A good agreement between measurements and models is found ~~for in~~ the 5 to 100 hPa profile, with GEOSCCM underestimating the vertical flux between 50 and 30 hPa. ~~In Fig. 2c we show a latitudinal breakdown~~ [Figure S4 in the supplementary material shows a latitudinal section](#) of the heat fluxes ~~averaged over the 1981-2002 period for the models and the reanalysis~~ in order to further evaluate the transport skill of the ~~models~~. ~~A greater agreement is found over the Southern Hemisphere at mid to high latitudes compared to the Northern Hemisphere, however both models fall inside 1 σ of the ERA40 20 years variability from 50° to 90° in both hemispheres.~~ [two models](#).

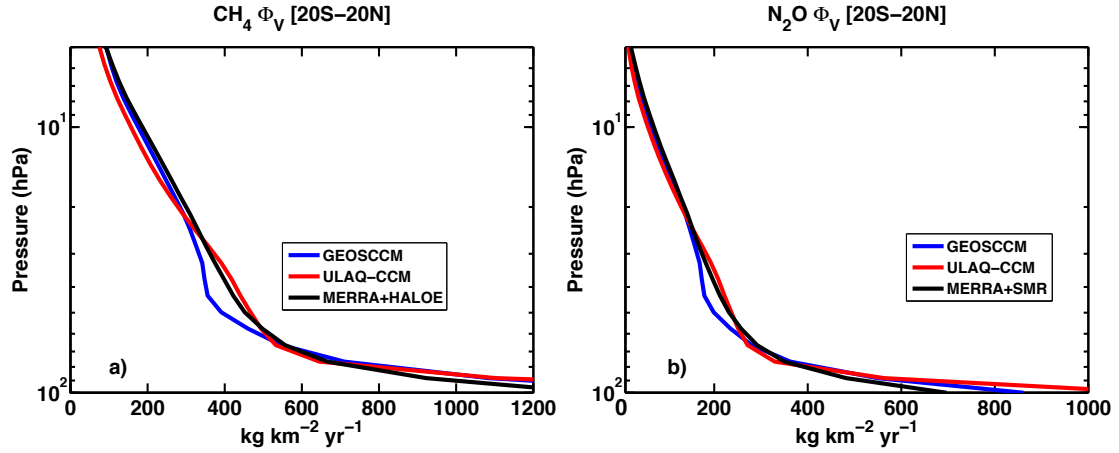


Figure 2. Tropical stratospheric vertical mass fluxes (20S-20N) of (a) CH_4 and (b) N_2O for GEOSCCM (blue) and ULAQ-CCM (red) results; the vertical mass fluxes are defined as $[\rho w^*]$, where w^* is the zonal mean residual vertical velocity and ρ is the zonally averaged mass concentration of CH_4 and N_2O , respectively. A model evaluation is made with flux data obtained with w^* from MERRA reanalysis and CH_4 , N_2O mixing ratios from HALOE and SMR results (black) ($\text{kg km}^{-2} \text{yr}^{-1}$). CH_4 and N_2O fluxes are averaged over 1991-2005 and 2001-2005, respectively, to keep consistency with the adopted HALOE and SMR mixing ratio values. Panel (c) presents an evaluation of 100 hPa horizontal eddy heat fluxes as a function of latitude averaged over 1981-2002 for the same two models (GEOSCCM in blue and ULAQ-CCM in red) with ERA40 reanalysis (Kms^{-1}). The eddy heat fluxes are averaged over winter months, i.e., for July and August in the Southern Hemisphere and January-February over the Northern Hemisphere and are defined as $\overline{v'T}$, where v is the 3D meridional wind component and T the temperature. The square brackets denote a zonal average and the prime a deviation from the zonal average.

4 Perturbation of Stratospheric Species Transport

Absorption of solar near-infrared (NIR) and planetary radiation by the geoengineering aerosols produces an increase of diabatic heating rates in the tropical lower stratosphere, resulting in local warming, changes in the latitudinal distribution of zonal winds, changes of the equatorial QBO (Aquila et al. (2014)) and a strengthening of the stratospheric Brewer-Dobson circulation (BDC) (Pitari et al. (2014)). Enhanced tropical upwelling (about 5-10% increase in vertical velocities in the lower stratosphere) and extra-tropical descent tend to move CH₄ poor air more efficiently towards the extra-tropical UTLS, as well as for other stratospheric long lived species. The net impact on tropospheric OH and CH₄ lifetime depends on the net result of superimposed species perturbations in the UTLS (CH₄, NO_y, O₃, SO₄), in addition to tropospheric chemistry perturbations due to changes in water vapor content, UV radiation and heterogeneous reactions on sulfate aerosols that affect the NO_x balance. The 5-10% increase of stratospheric tropical upward mass fluxes of both CH₄ and N₂O, as shown in Fig. 3ab, is predicted by the models in geoengineering conditions, as a consequence of the increasing tropical mid-stratospheric upwelling, with a larger anomaly in GEOSCCM with respect to both MBC experiments run with the ULAQ-CCM (cases (a) and (c) in Table 1, with 8 and 5 Tg-SO₂ injected, respectively). The choice to only include MBC experiments when discussing vertical mass flux anomalies is made in order to better highlight transport anomalies, because in the FBC experiment the anomaly would be largely masked by the increasing amount of tropospheric CH₄. The larger GEOSCCM anomaly could be explained by the QBO modification produced by geoengineering aerosols, since the prolonged lower stratospheric westerly phase produces a better tropical confinement (Trepte and Hitchman (1992); Aquila et al. (2014); Visoni et al. (2017)). This effect is absent in the ULAQ-CCM model, which does not have an internally generated QBO, but specifies the QBO with observed equatorial zonal wind data using a nudging procedure (Morgenstern et al. (2010)).

The UTLS horizontal mixing anomalies (Fig. 3cd) are larger in case (a) of ULAQ-CCM with respect to ULAQ-CCM (c) and GEOSCCM. In the latter two model simulations, ~~SSTs in G4 are the same as in RCP4.5~~ SSTs are used for both the baseline and the geoengineering perturbed experiments, whereas ULAQ-CCM (a) is driven ~~by SSTs taken from an atmosphere-ocean coupled model run in geoengineering conditions (i.e., in the latter experiment by G4 surface temperatures (from CCSM-CAM4)~~. In this case, the larger decrease of the UTLS horizontal mixing can be explained by the increased atmospheric stabilization caused by the sea surface cooling, which is not present in GEOSCCM and ULAQ-CCM (c), ~~where SSTs in G4 are unchanged with respect to RCP4.5~~. The ULAQ-CCM (c) results do not change significantly in a sensitivity simulation made increasing the stratospheric sulfur injection from 5 Tg-SO₂/yr to 8 Tg-SO₂/yr (see Table ??2), pointing out to the important role of the decreasing horizontal mixing resulting from sea surface cooling, as in ULAQ-CCM (a).

The time series of model calculated CH₄ and N₂O changes in the UTLS is presented in Fig. 4 for ULAQ-CCM and GEOSCCM. If we compare the ULAQ-CCM case (c) with GEOSCCM, the results of the two models are similar for N₂O and are consistent with changes of lower stratospheric heating rates and BD circulation (due to aerosols and O₃). The N₂O anomalies are of the order of -1 ppbv in both models (that is about -0.3%), while those of CH₄ are of the order of -5 ppbv in the ULAQ model and about a factor of 2 smaller in GEOSCCM. This is due to missing chemical processes in the upper

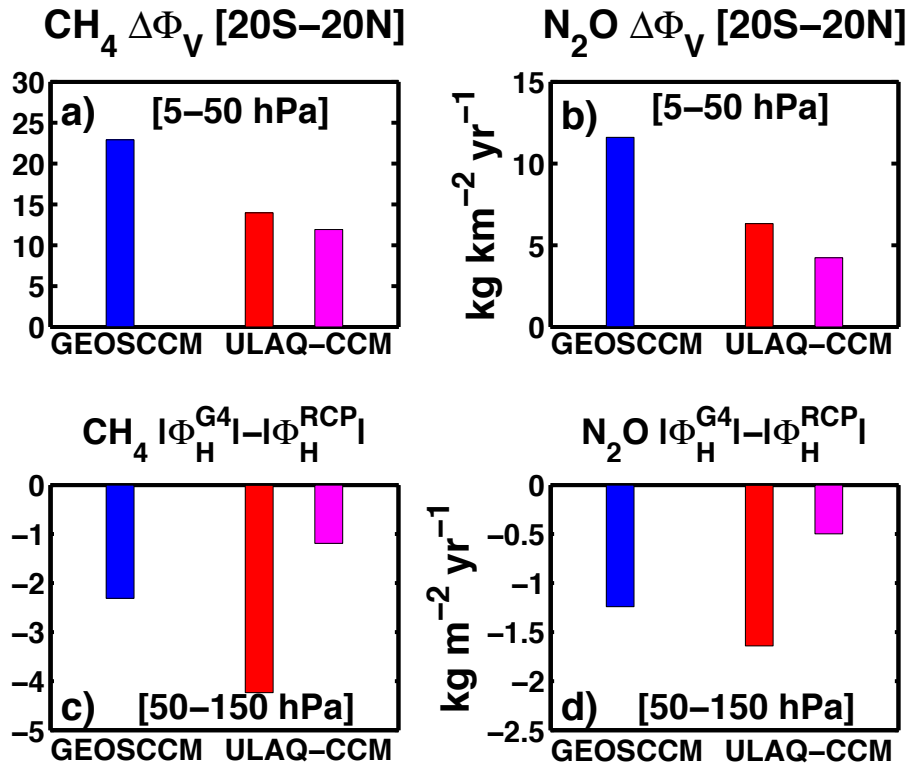


Figure 3. G4-RCP4.5 anomalies of (a,b) vertical and (c,d) horizontal mass fluxes of (a,c) CH₄ and (b,d) N₂O (years 2040-49 time average). Vertical mass fluxes in panels (a,b) (defined as in Fig. 2) are averaged over the tropics (20S-20N) in the 5-50 hPa vertical layer, with GEOSCCM results in blue and ULAQ-CCM results in red and magenta for cases (a) and (c) as in Table 1, respectively (kg km⁻² yr⁻¹). Horizontal mass fluxes in panels (c,d) (defined as $v\rho$, with v and ρ the 3D meridional wind component and mass concentration of CH₄ and N₂O, respectively) are averaged (in absolute values) over the extra-tropics (90S-20S and 20N-90N) in the 50-150 hPa vertical layer, with model results as in panels (a,b) (kg m⁻² yr⁻¹).

troposphere in GEOSCCM, where tropospheric OH is kept fixed at RCP4.5 values.

As already discussed in Fig. 3, the UTLS anomalies G4-RCP4.5 are rather different for ULAQ-CCM (a), mostly as a consequence of the changing SSTs in G4, with decreased horizontal mixing in the UTLS and enhanced isolation of the tropical pipe. The negative anomaly of N₂O (a quasi-passive tracer) increases up to 2-4 ppbv after 2030, whereas the negative CH₄ anomaly increases up to approximately 10 ppbv between 2030 and 2050. A clear sign inversion is predicted after 2050 for the CH₄ anomaly in geoengineering conditions, as a consequence of a negative OH trend resulting from superimposed effects of NO_x and O₃. A positive trend of stratospheric O₃ is, in fact, predicted in G4 with respect to RCP4.5 due to the lowering chlorine-bromine loading in the atmosphere [in the 21st century](#) (Pitari et al. (2014)).

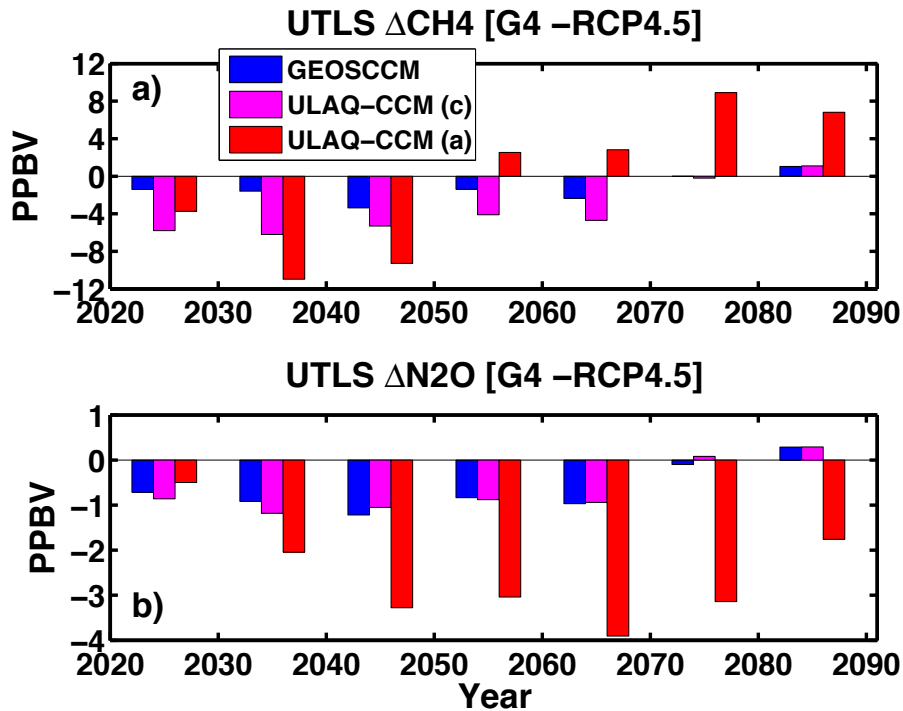


Figure 4. Time series of globally averaged changes of CH₄ (a) and N₂O (b) in the 50-150 hPa vertical layer, for GEOSCCM (blue) and ULAQ-CCM (red and magenta, for cases (a) and (c) as in Table 1, respectively) (decadal averages). Units are ppbv.

The zonally averaged changes of N₂O and CH₄ are presented in Fig. 5, with a comparison of model results from GEOSCCM and ULAQ-CCM (a). The mid-stratospheric changes are quite comparable between the two models, whereas the UTLS negative anomalies in ULAQ-CCM (a) are significantly larger for the reasons discussed above in Fig. 3-4, whereas they are fully comparable when considering GEOSCCM and ULAQ-CCM (c) results, [as shown in Fig. S5](#). Again, this points out to the sea surface cooling role on the UTLS horizontal mixing in sulfate geoengineering conditions. [Further remaining differences](#)

5 [between GEOSCCM and ULAQ-CCM \(c\) regarding horizontal mixing can be explained by a different treatment of QBO, which is in GEOSCCM modified with a prolonged E-shear in the G4 simulation. Inter-hemispheric asymmetries in the lower stratospheric mixing ratio anomalies of ULAQ-CCM \(a\) and their differences with respect to GEOSCCM can be explained by a combination of vertical and horizontal mass flux changes, and will be addressed later on in the discussion.](#)

To better understand the differences between the cases with fixed SSTs and the one with changing SSTs, in Fig. 6 we show

10 the [anomalies in sea surface temperatures used in ULAQ-CCM \(a\) and \(b\) ,which against the ones used in ULAQ-CCM \(c\); surface temperatures](#) are taken from the CCSM-CAM4 ocean-atmosphere coupled model for RCP4.5 and G4 simulations (with injection of 8 Tg-SO₂). ~~The time series of the globally averaged surface temperature anomalies is shown in Fig. 6a for the RCP4.5 and G4 cases: the slow oceanic response coupled to the atmospheric perturbation of long lived species delays by approximately 20 years the surface temperature return in G4 to RCP4.5 values.~~ [as described in Table 2](#). The zonally averaged

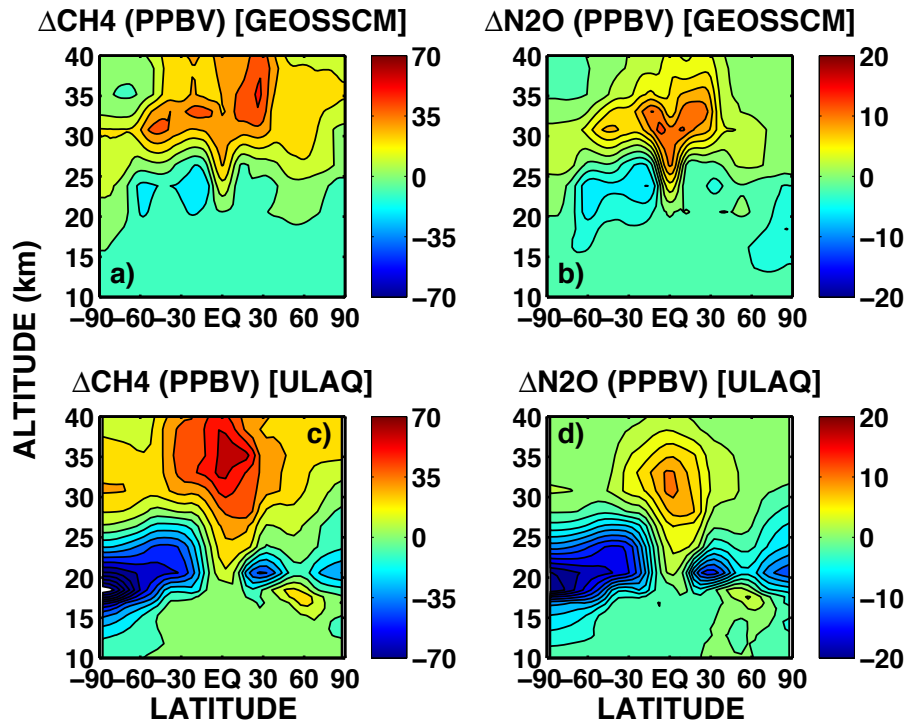


Figure 5. Zonal mean mixing ratio anomalies G4-RCP4.5 for (a,b) GEOSCCM and (c,d) ULAQ-CCM, for CH₄ (a,c) and N₂O (b,d) (time average 2040-2049). ULAQ-CCM results are for case (a) in Table 1. Units are ppbv. In panels (a,c) the contour line increment is 10; in panels (b,d) the contour line increment is 2.

- 15 surface temperature anomalies G4-RCP4.5 are presented in Fig. 6b-a for the various decades from 2020 to 2090. A strong inter-hemispheric asymmetry is evident, with a negative anomaly more pronounced in the Arctic region by approximately 1.5 K with respect to the latitude range 50S-70S. The geoengineering cooling impact on Arctic sea ice is the main driver for the larger negative temperature anomaly in the Northern Hemisphere high latitudes, which favors a more pronounced atmospheric stabilization in the Northern Hemisphere winter-spring months with respect to the Southern Hemisphere. [The time series of the globally averaged surface temperature anomalies is shown in Fig. 6b for the RCP4.5 and G4 cases; the slow oceanic response coupled to the atmospheric perturbation of long lived species delays by more than one decade the surface temperature return in G4 to RCP4.5 values.](#)

The decreased horizontal fluxes of long lived species discussed in Fig. 3 for the ULAQ-CCM simulations with changing SSTs are a direct consequence of the atmospheric stabilization. As shown in Fig. 6c, the increased atmospheric stability in sulfate geoengineering conditions may be partially counterbalanced by the increased longitudinal variability of the induced cooling, in particular in the Northern Hemisphere, which may enhance the amplitude of planetary waves. Regions of oceanic warming in the sub-Arctic are a consequence of the increasing amount of sea ice in G4 and related enhanced transport of colder and saltier waters towards the subpolar regions (Tilmes et al. (2009)). This favors cold sea water downwelling and thus positive anomalies

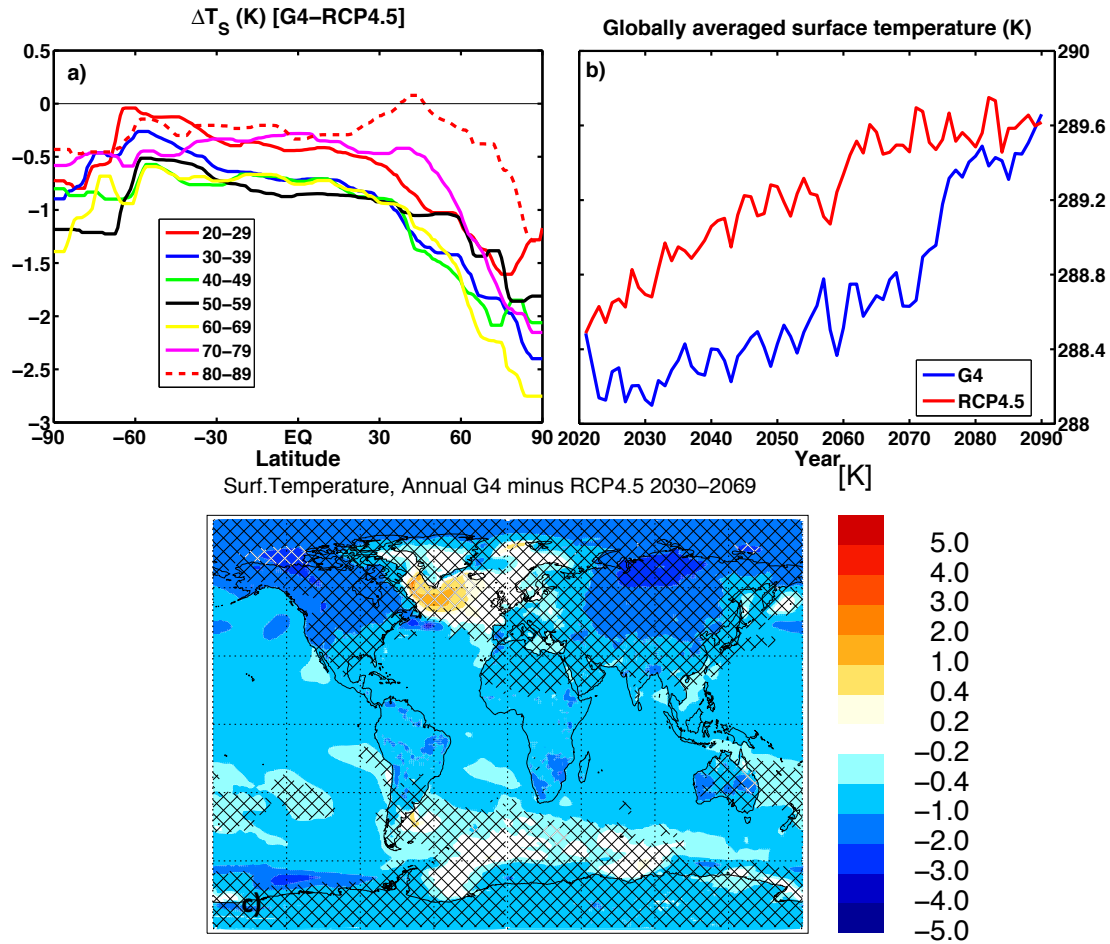


Figure 6. Panel (a): zonally averaged surface temperature changes G4-RCP4.5 (K) in the ULAQ-CCM (cases (a) and (b)), using sea surface temperatures from the atmosphere-ocean coupled model CCSM-CAM4 (decadal time averages from year 2020 to ~~2080~~2089; see legend for the different colors). Panel (b): time series of the globally averaged surface temperatures (K) from year 2020 to 2090 (RCP4.5 in red and G4 in blue). Panel (c): annually averaged surface temperature anomalies G4-RCP4.5 (K), from the atmosphere-ocean coupled model CCSM-CAM4 (time average 2030-2069). Shaded areas are not statistically significant within $\pm 1\sigma$.

of SSTs with respect to reference RCP4.5 conditions, mainly in the North Atlantic region (where the decrease of sea ice would produce less saltier waters, followed by less downwelling, leading to cooler SSTs).

Lastly, we show the anomalies of vertical and horizontal fluxes in Fig. 7 and Fig. 8, respectively, for ULAQ-CCM (a) and for GEOSCCM. For ULAQ-CCM (a), a 5% increase of the mid stratospheric tropical upward fluxes is predicted in G4 with respect to the reference RCP4.5 case, with a pronounced inter-hemispheric asymmetry. The Southern Hemisphere increase of downward mass fluxes is much larger than in the Northern Hemisphere, both in absolute and relative units. The stratospheric

mean meridional circulation is more efficiently perturbed in the Southern Hemisphere, due to the more effective atmospheric stabilization in the Northern Hemisphere (see above Fig. 6). A 5-10% decrease of the extra-tropical horizontal mass fluxes is also predicted, as expected from the discussion above for Fig. 6. The isolation of the tropical pipe is increased in a dynamical regime with increased tropical upwelling and enhanced atmospheric stabilization. The importance of SSTs changes due to geoengineering is highlighted by the much smaller ~~hemispheric-inter-hemispheric~~ difference shown by ~~the GEOSCCM model~~ GEOSCCM for the downward fluxes, as well as in ULAQ-CCM (c) (not shown), while the increase in the tropical upward fluxes in Fig. 7 is comparable to the ULAQ-CCM results. Due to less atmospheric stabilization, furthermore, ~~in Fig. 8 the GEOSCCM model-GEOSCCM~~ shows much smaller changes in extratropical horizontal fluxes ~~-(Fig. 8). This is further highlighted in Fig. S6, where the horizontal mass flux anomalies are also shown for ULAQ-CCM (c). In this figure, the difference between the two ULAQ-CCM simulations regarding the horizontal mass flux anomalies is clearly visible, with ULAQ-CCM (c) having latitudinal means one order of magnitude smaller compared to ULAQ-CCM (a), and much more comparable to GEOSCCM in the extratropics.~~

5 Another highlight of the different effects of transport and chemical effects on ~~the lifetime~~ lifetimes is shown in Table 4, where atmospheric lifetime anomalies are shown for five species with stratospheric photolysis and ~~O(¹D)~~ O(¹D) reaction, as calculated in ULAQ-CCM (b). The net lifetime changes G4-RCP4.5 result from the superposition of two effects: perturbation of species transport and sulfate aerosol induced changes in O₃ via NO_x depletion from heterogeneous chemical reactions. The increased tropical upwelling moves more efficiently these long lived species at higher altitudes in the mid stratosphere where

10 the photolysis sink is enhanced, thus decreasing the lifetimes. On the other hand, the chemically induced ozone increase (due to the NO_x sink by sulfate aerosols) tends to increase the overhead column, with a decreased mid-stratospheric UV flux. As a consequence, the photolysis rates decrease, thus prolonging the lifetimes. As shown in Pitari et al. (2014), however, the net effect on ozone of the aerosol induced NO_x depletion is not constant in time, due to the decreasing amount of Cl-Br species during the 21st century.

15

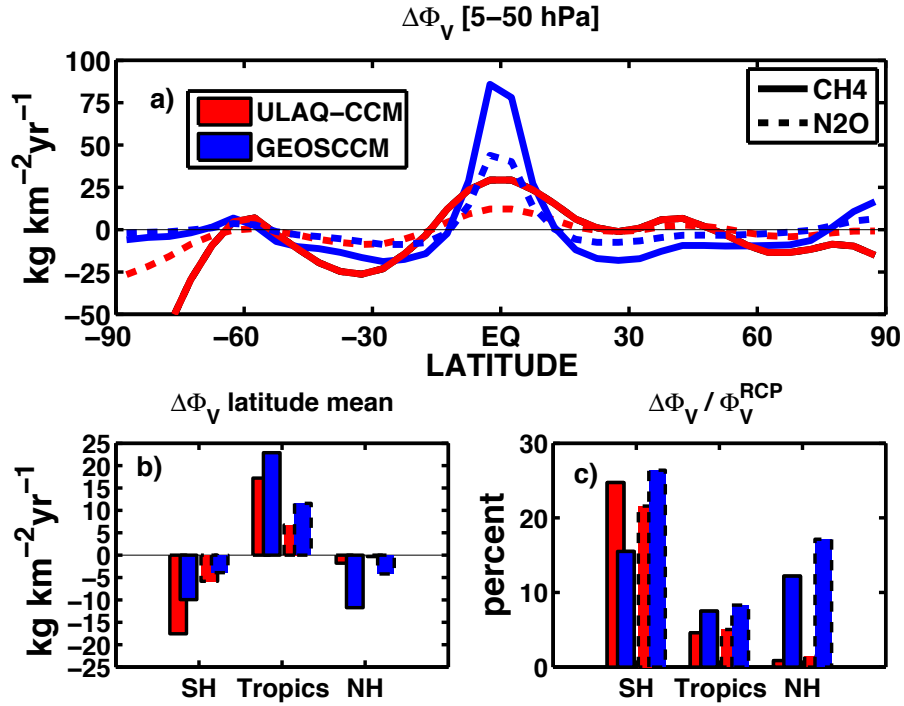


Figure 7. Panel (a): latitude dependent CH_4 (solid line) and N_2O (dashed line) vertical mass flux anomalies G4-RCP4.5 from the ULAQ-CCM (a) and GEOSCCM calculations, in red and blue respectively (vertical average 5-50 hPa; time average 2040-2049). Units are $\text{kg km}^{-2}\text{yr}^{-1}$. Panels (b) and (c) show the corresponding latitude averaged mass flux anomalies (absolute and percent values, respectively): SH from 90S to 20S; Tropics from 20S to 20N; NH from 20N to 90N. The vertical flux anomalies $\Delta\Phi_V$ are defined as $\Delta[w^* \rho_{\text{CH}_4}^{\text{RCP4.5}}]$ and $\Delta[w^* \rho_{\text{N}_2\text{O}}^{\text{RCP4.5}}]$, where w^* is the zonal mean residual vertical velocity, $\rho_{\text{CH}_4}^{\text{RCP4.5}}$ and $\rho_{\text{N}_2\text{O}}^{\text{RCP4.5}}$ are the mass concentrations of CH_4 and N_2O , respectively, and Δ denotes the G4-RCP4.5 difference.

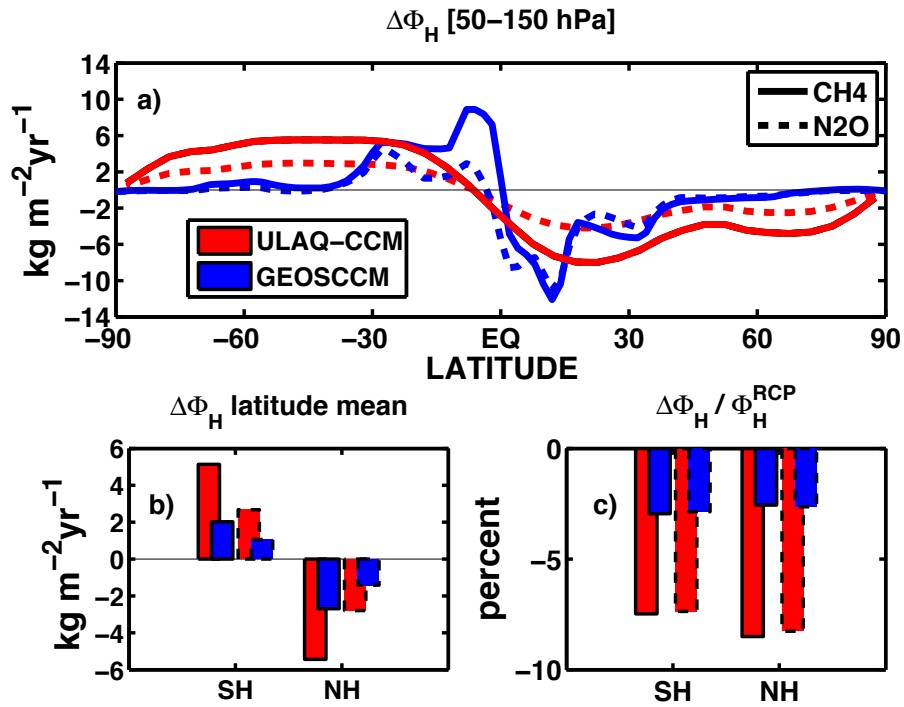


Figure 8. As in Fig. 7, but for horizontal mass flux anomalies G4-RCP4.5 (vertical average 50-150 hPa; time average 2040-2049). Units are $\text{kg m}^{-2} \text{yr}^{-1}$. The horizontal flux anomalies $\Delta\Phi_H$ are defined as $\Delta[v\rho\text{CH}_4]$ and $\Delta[v\rho\text{N}_2\text{O}]$, where v is the 3D meridional wind component.

Table 4. Atmospheric lifetimes (years) calculated in the ULAQ-CCM (case (b) in Table 1), relative to five species with stratospheric photolysis and O(¹D) reaction sink (i.e., N₂O, CFC-11, H1301, CFC-12, CFC-114). First column shows year 2000 values (as an average over the 1996-2005 decade); second column shows a model mean from the SPARC (2013) report on lifetimes. Subsequent columns show the calculated lifetime anomalies due to sulfate geoengineering (average 2030-2069). Inside the square brackets we highlight the physical and chemical effects driving the lifetime changes: changing stratospheric transport in the fourth column and changing stratospheric O₃ in the fifth column (due to the aerosol induced NO_x loss). Results in the rightmost two columns are obtained through G4 sensitivity experiments (sn1, sn3) explained in Table 2.

	1996-2005	Model Mean [SPARC, 2013]	2030-2069 G4-RCP4.5 [All effects]	2030-2069 G4-G4[sn3] [Transport]	2030-2069 G4[sn1]-RCP4.5 [NO _x → O ₃ → UV]
N ₂ O	116.1	115.0 ± 9.0	-0.4	-3.0	+2.6
CFC-11	52.2	55.3 ± 4.2	+2.2	-0.2	+2.4
H1301	77.9	73.4 ± 4.7	+1.1	-1.4	+2.6
CFC-12	92.0	94.7 ± 7.3	-0.1	-2.7	+2.6
CFC-114	202	189 ± 18	-2.3	-4.9	+2.6

5 Perturbation of Tropospheric Chemistry

Stratosphere-troposphere exchange of geoengineering sulfate enhances the aerosol SAD in the upper troposphere, thus favoring NO_x depletion through heterogeneous chemical reactions (i.e., hydrolysis of N₂O₅ and $\text{BrONO}_2 \rightarrow \text{BrONO}_2$) (Tilmes et al. (2009)). Again, this implies less OH production and a longer CH₄ lifetime (mostly via NO + HO₂ → NO₂ + OH). Fig. 9 compares the G4-RCP4.5 anomalies of sulfate aerosol mass and surface area density in the UTLS, as calculated in ULAQ-CCM (c) and GEOSCCM. The ULAQ-CCM model results are taken from numerical experiments (c) in Table 1 in order to make a more meaningful comparison with GEOSCCM (same injection of 5 Tg-SO₂/yr, SSTs in G4 with respect to RCP4.5). The ULAQ model results are taken from numerical experiments (c) in Table 1 in order to make a more meaningful comparison with GEOSCCM (same injection of 5 Tg-SO₂/yr, SSTs in G4 with respect to RCP4.5).

A combination of isentropic SO₄ transport above the tropopause and tropical upwelling/extratropical descent produces aerosol accumulation in the extratropical lower stratosphere with a clear maximum of mass density in the Northern Hemisphere (>2 μgm⁻³ at ~12-14 km altitude). Larger values in the ULAQ-CCM of both SAD and mass density in the tropical upper troposphere are due to a more efficient gravitational settling of the particles. An important difference between the two models is that ULAQ-CCM includes an aerosol microphysical-microphysics code for predicting the particle size distribution, which, on the other hand, is assigned in GEOSCCM (Pitari et al. (2014)). A similar increase of SAD is predicted by both models in the extratropical upper troposphere. A comparison of the simulated stratospheric distribution of the SO₄ SAD is shown in Fig. S7 in order to highlight the ability of both models to correctly simulate the tropical aerosol confinement, and a further

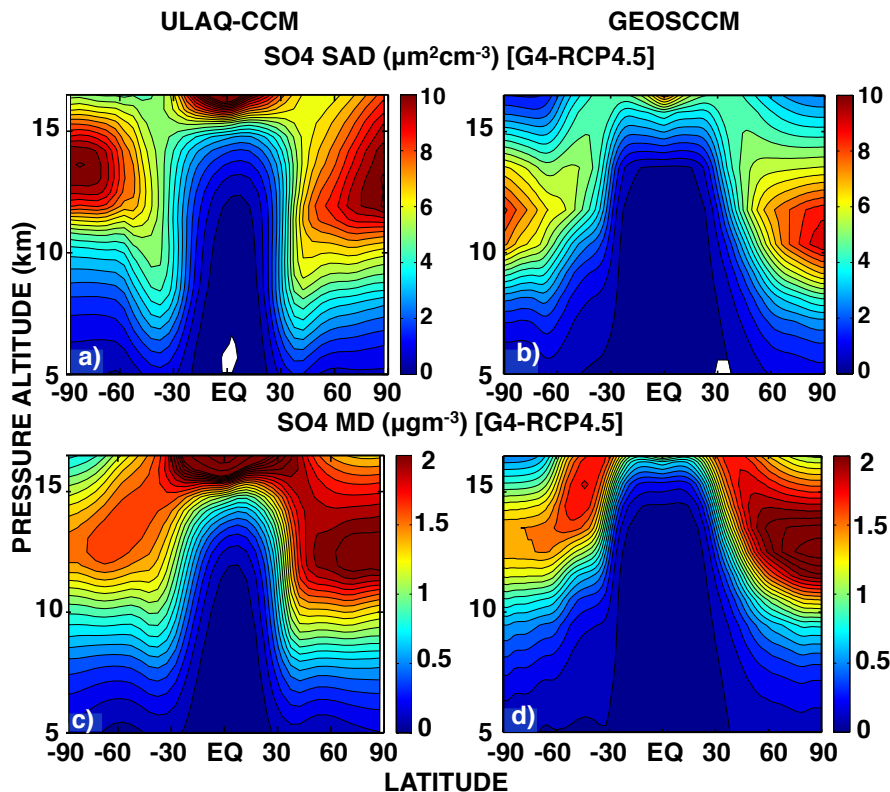


Figure 9. G4-RCP4.5 anomalies of sulfate aerosol surface area density (a,b) and mass density (c,d) in the upper troposphere and lowermost stratosphere, from ULAQ-CCM (a,c) and GEOSCCM (b,d) (time average 2040-2049). ULAQ-CCM results are from numerical experiments (c) in Table 1. Units are $\mu\text{m}^2\text{cm}^{-3}$ for the surface area and μgm^{-3} for the mass density. In panels (a,b) the contour line increment is 0.5 for values less than 12 and 2.0 from 14 to larger values. In panels (c,d) the contour line increment is 0.1 for values less than 2.5 and 1.0 from 3.0 to larger values.

[discussion of the differences between the two models in this aspect, together with profile evaluation using SAGE II data, is presented in Pitari et al. \(2014\).](#)

10 [The two models predict an increase of SAD ranging between 2 to 10 \$\mu\text{m}^2\text{cm}^{-3}\$. The upper tropospheric increase of sulfate aerosol surface area density in the extratropical upper troposphere, and this increase](#) is the major driver for tropospheric NO_x changes in geoengineering conditions. Enhanced heterogeneous NO_x conversion to HNO_3 on the aerosol surface ends up limiting the efficiency of reaction $\text{NO} + \text{HO}_2 \rightarrow \text{NO}_2 + \text{OH}$, thus reducing OH and upper tropospheric O_3 production, with a consequently longer CH_4 lifetime. Fig. 10 shows the ULAQ model calculated anomaly of UTLS NO_x in experiment (b) of Table 1, with values ranging between -0.02 and -0.2 ppbv in the upper troposphere (10 to 30% reduction).

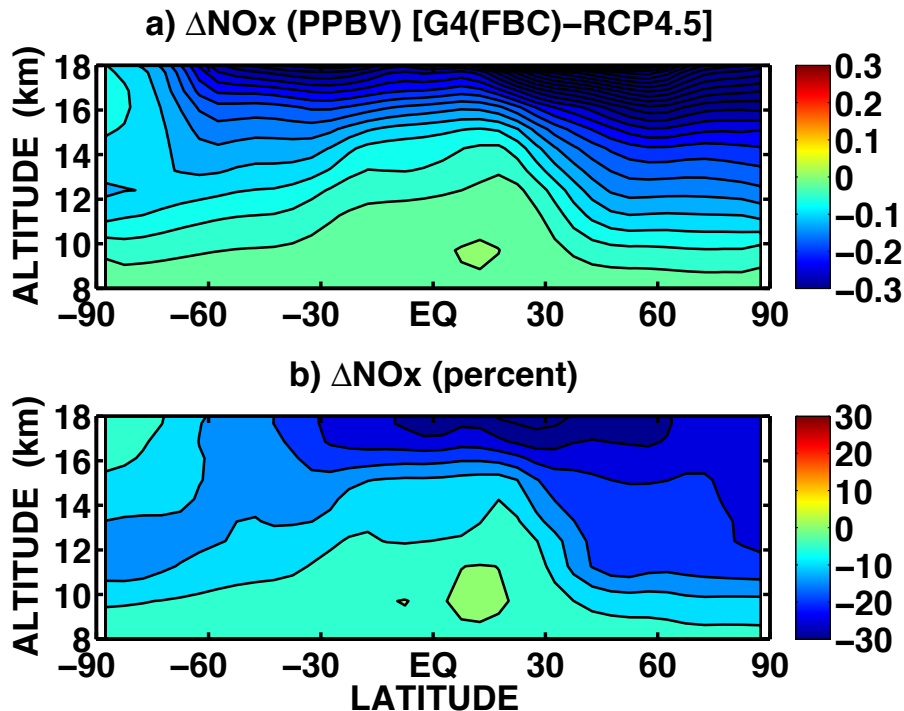


Figure 10. G4-RCP4.5 anomalies of NO+NO₂ mixing ratios in the upper troposphere and lowermost stratosphere, from experiment (b) of the ULAQ-CCM (time average 2040-2049). Panels (a,b) are for absolute (ppbv) and percent NO_x changes, respectively. The contour line increments are 0.025 ppbv and 5%, in panels (a,b) respectively.

The tropospheric OH balance is also affected also by the UV amount available for O(¹D) production from O₃ photolysis (H₂O + O(¹D) → 2OH), and indirectly from the upper tropospheric O₃ reduction due to the decreased chemical production from NO+HO₂ and NO+RO₂. Upper tropospheric ozone, however, is also affected by perturbed strat-trop fluxes and lower stratospheric ozone depletion in geoengineering conditions (Pitari et al. (2014); Xia et al. (2017)). High latitude stratospheric ozone depletion produces significant UVB increase at the surface (Tilmes et al. (2012)). On the other hand, the enhanced radiation scattering in the tropical lower stratosphere overbalances the UVB increase due to tropical stratospheric ozone losses, ending up in a net decrease of tropical tropospheric UVB, ~~that is which means~~ again less OH production and longer CH₄ lifetime (~~which is mostly regulated~~ regulated essentially by tropical OH). Fig. 11 shows the percent anomalies of UVB as calculated in GEOSCCM and ULAQ-CCM (c), for the two components that are explicitly on-line in the models (O₃ and sulfate aerosols). A 1.5 ~~÷to~~ to 2.0% UVB decrease is predicted by the models equatorward of 40° latitude in both hemispheres (-1.60% for GEOSCCM and -1.94% for ULAQ-CCM). The sulfate geoengineering impact on tropospheric UV penetration and heterogeneous chemistry changes have been widely discussed in Xia et al. (2017), along with their effects on surface ozone concentration.

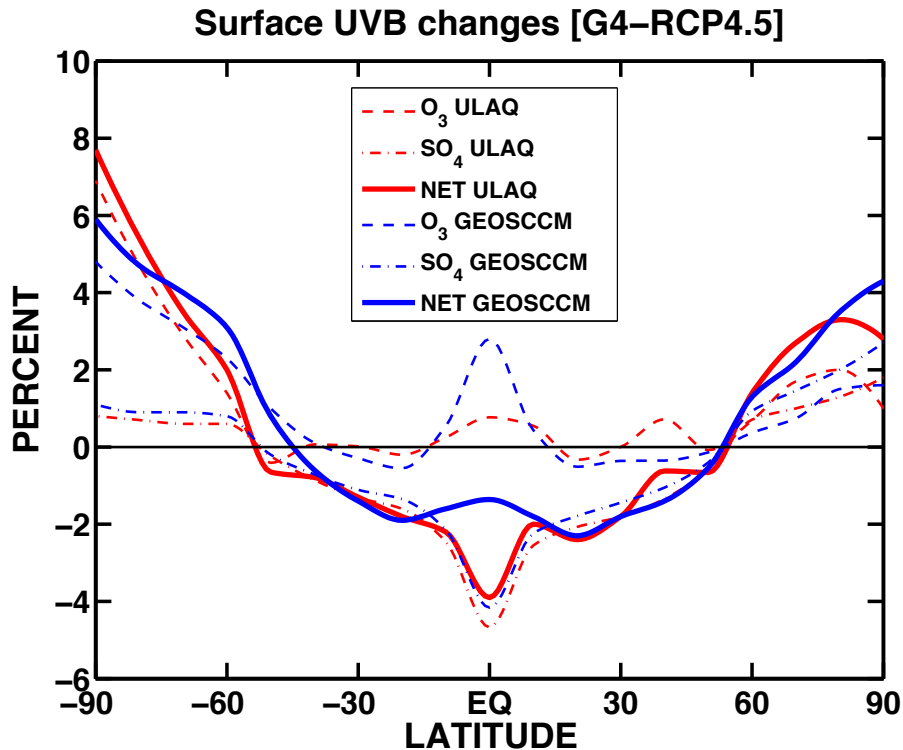


Figure 11. G4-RCP4.5 percent anomalies of surface UVB as a function of latitude, from ULAQ-CCM (c) (red) and GEOSCCM (blue) (2040-2049). UVB changes are shown for the two components that are explicitly on-line in the models (i.e., O₃ and aerosols) and for their net. ULAQ-CCM results are taken from numerical experiment (c) in Table 1 in order to make a more meaningful comparison with GEOSCCM, as in Fig. 12.9.

Solar radiation scattering reflection by geoengineering aerosols increases the planetary albedo and cools the surface, with a tropospheric water vapor decrease as a response to this cooling: less OH is produced by reaction $\text{H}_2\text{O} + \text{O}(^1\text{D})$, thus prolonging the CH₄ lifetime. The combination of this climate-chemistry effect with the others discussed above (NO_x, UV, strat-trop O₃ transport) produces the net OH perturbation in G4 with respect to RCP4.5 (Fig. 12a) and the resulting CH₄ change (Fig. 12b). The calculated average tropospheric anomaly of CH₄ is +190 ppbv, that is 10.6% with respect to the RCP4.5 base case average mixing ratio in years 2040-2049. The stratospheric anomalies are consistent with those discussed in Fig. 5c, obtained with the same G4 perturbation, but using the MBC approach (ULAQ-CCM (a)).

Any attempt to assess the long-term atmospheric response of CH₄ to OH changes needs the surface mixing ratio to be allowed to respond freely to tropospheric perturbations of its main sink process (i.e., oxidation by OH), which determines the CH₄ lifetime. The usual modeling approach of adopting an assigned time-dependent mixing ratio as a surface boundary condition (MBC) can still be used to calculate climate-chemistry induced changes in CH₄ lifetime, but this cannot provide in-

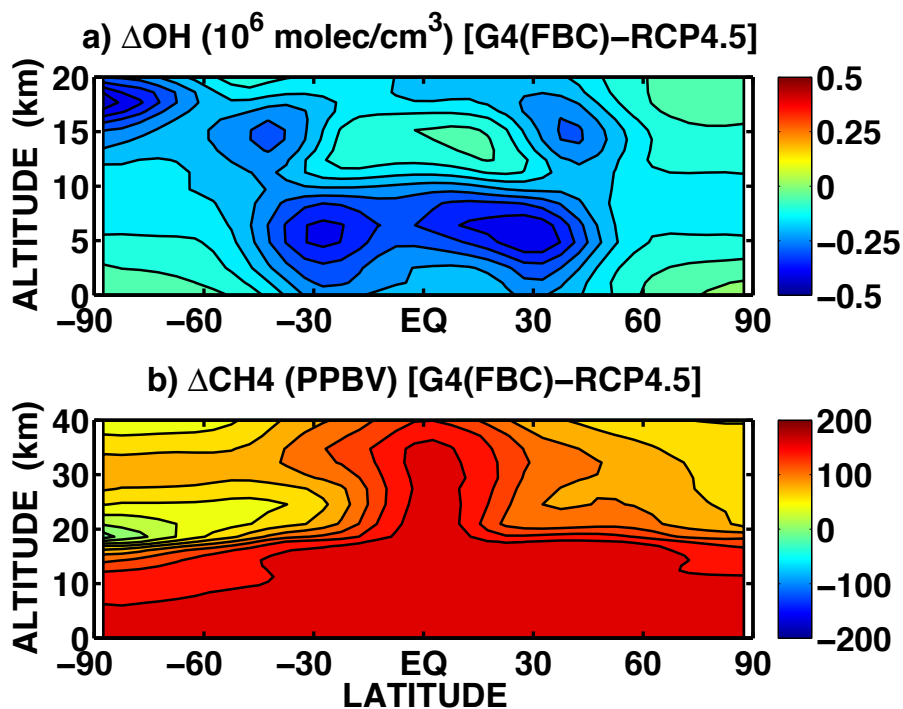


Figure 12. ULAQ-CCM calculated G4-RCP4.5 anomalies of (a) OH concentrations and (b) CH₄ mixing ratios (time average 2040-2049), from experiment (b) in Table 1. Units are 10^6 molec/cm^3 for OH and ppbv for CH₄. The contour line increment is $0.1 \times 10^6 \text{ molec/cm}^3$ for OH and 25 ppbv for CH₄.

formation on the tropospheric mass changes of CH₄ induced by the OH perturbations. In addition, to obtain a correct estimate of the lifetime perturbation, the MBC approach would necessitate the use of correction factors, due to the missing feedback of lower tropospheric CH₄ changes on HO_x chemistry (Myhre et al. (2011)).

Table 5. CH₄ surface emissions, sinks, global mass burden and lifetime in the ULAQ-CCM for experiment (b) (year 2000). (a) IPCC (2013); (b) Wecht et al. (2014); (c) Lamarque et al. (2010).

Emissions (Tg/yr) Sinks (Tg/yr) Burden (Tg) Lifetime (yr)	ULAQ-CCM [FBC]
Natural sources	230 ^(a,b)
[wetlands]	160 ^(a,b)
[termites]	20 ^(a,b)
[geological]	50 ^(a)
Anthropogenic sources	340 ^(a,c)
[agriculture]	125 ^(a,c)
[fossil fuel]	100 ^(a,c)
[waste]	79 ^(a,c)
[biomass burning]	36 ^(a,c)
Total sources	570 ^(a,c)
Soil deposition	30 ^(a)
Atmospheric loss [OH O(¹ D) Cl]	540
Total sinks	570
Global mass burden	4760
Atmospheric lifetime	8.8
Global lifetime	8.35

The alternative approach of using a surface flux boundary condition (FBC) would in principle resolve these issues. Table 5 summarizes CH₄ surface emissions, sinks, global mass burden and lifetime in ULAQ-CCM (b), for year 2000. The major atmospheric sink of CH₄ is the reaction with OH and this determines the CH₄ lifetime, except for an additional smaller contribution from soil deposition and an additional stratospheric sink due to CH₄ reactions with O(¹D) and Cl. The calculated OH abundance is then critical in the determination of a realistic global burden and lifetime of CH₄. Tropospheric OH concentrations have been evaluated in Pitari et al. (2016a) using climatological values from Spivakovsky et al. (2000). In the same published work, a comparison of calculated tropospheric CH₄ mixing ratios is made with observations from TES/Aura radiances.

The ULAQ-CCM calculated time series of CH₄ lifetime and surface mixing ratio is presented in Fig. 13a, for both reference RCP4.5 and perturbed G4 cases, using the FBC approach (experiment (b) in Table 1). A simple approach was used for the time evolution of CH₄ emission fluxes: the geographical distribution was fixed at year 2000 values, but the net global value was linearly scaled to the ratio of RCP4.5 recommended surface mixing ratios in future years (dotted line in Fig. 13a) with

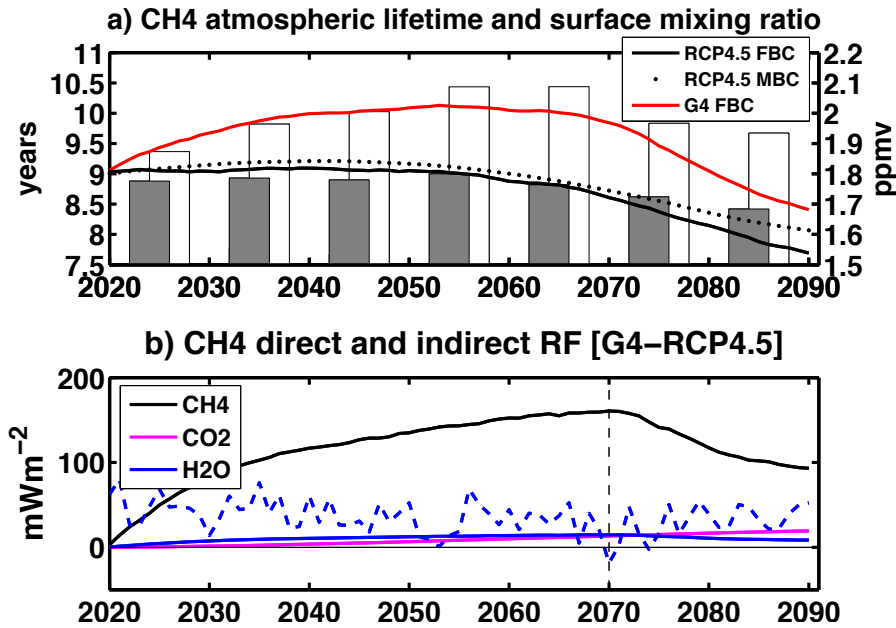


Figure 13. Panel (a): time series of CH₄ global mean atmospheric lifetime (years, left scale, bars) calculated in the ULAQ-CCM FBC case (experiment (b) of Table 1), with bars referring to decadal averages (gray for RCP4.5 and white for G4). Superimposed are globally averaged CH₄ surface mixing ratios (ppmv, right scale), for the corresponding RCP4.5 and G4 simulations (black solid and red curves, respectively). The dotted curve shows globally averaged CH₄ surface mixing ratios, for the RCP4.5 MBC case (experiment (a) in Table 1), i.e., using prescribed fixed mixing ratios at the surface (Eyring and et al. (2013)). Panel (b): time series of G4-RCP4.5 radiative forcing of CH₄ (mW/m²). Black, purple and blue curves show the direct and indirect effects (purple and blue curves are for CO₂ and stratospheric H₂O from CH₄ oxidation, respectively). Dashed blue curve is for stratospheric H₂O changes resulting from G4-RCP4.5 temperature anomalies at the TTL.

5 the year 2000 recommended value (1754 ppbv). An in-depth study of future climate change effects on CH₄ natural emissions or future changes on the geographical distribution of anthropogenic emissions τ is beyond the purposes of the present study. The lifetime change G4-RCP4.5 shown in Fig. 13a increases up to 1.7 years in 2070 during the time period of geoengineering implementation, then slowly decreases in the so-called termination period (2070-2090), down to 1.2 years in 2090. Similarly, the surface mixing ratio change increases up to 250 ppbv in 2070 and then slowly decreases in the termination period, down to 150 ppbv in 2090. These slow decreases are due to the long time needed for atmospheric CH₄ to return to baseline RCP4.5 values. In addition, sea surface temperatures need a few decades to recover to RCP4.5 values (Fig. 6ab), thus triggering a
 10 prolonged perturbation of the stratospheric circulation.

A summary of gas phase RF components related to the CH₄ perturbation is presented in Fig. 13b. Direct stratospheric aerosol RF obviously dominates in sulfate geoengineering (~ -1.2 W/m²), as discussed in Visioni et al. (2017), using independent
 15 estimates available in literature. Among gas species CH₄ produces the largest indirect RF ($\sim +0.1$ W/m²), in addition to con-

tributions from O₃ (negative) and stratospheric H₂O (positive), the latter due to slight warming of the tropopause tropical layer (TTL) (see Pitari et al. (2014)). Small indirect CH₄ contributions come from increasing amounts of CO₂ and H₂O in the CH₄ oxidation chain. This chemical increase of stratospheric H₂O, however, is normally smaller than the one driven by the geoengineering aerosol warming at the TTL cold point (as shown in Fig. 13b).

20 Table 6 summarizes our calculations for OH-dependent species lifetimes under geoengineering conditions. The ULAQ-CCM calculated lifetimes under year 2000 conditions are fully comparable with the values in the SPARC (2013) report on lifetimes. G4-RCP4.5 anomalies averaged between 2030-2070-2030-2069 range between +1.33 years for CH₄ to +0.5 years for CH₃CCl₃ and +0.1 years for CH₃Br and CH₃Cl. The FBC approach was used for CH₄ in order to properly evaluate its feedback on HO_x chemistry. The rightmost three columns in Table 6 show the different contributions to the lifetime changes, through G4 sensitivity experiments (sn1, sn2, sn3) explained in Table 2. The major contribution to the CH₄ lifetime change (but also

5 for HCFC-22 and CH₃CCl₃) come from the presence of aerosols with their feedback on NO_x-HO_x-O₃ photochemistry, as discussed before with Fig. 9-10-11 (temperature and winds are kept unchanged with respect to RCP4.5 in the G4-sn1 sensitivity case, in the chemistry module and continuity equations of chemical tracers).

The effects of tropospheric cooling with decreased water vapor (due to solar radiation scattering by the stratospheric aerosols) and strengthening of the BDC with enhanced strat-trop downward flux (due to heating rates by the stratospheric aerosols) tend

10 to partially or completely cancel each other. The impact of tropospheric cooling on OH-driven lifetimes is limited by the fact that the lowered H₂O and OH production is partially counterbalanced by a less efficient reaction NO+O₃ → NO₂+O₂ in a colder troposphere -(see Fig. S8). This decreases NO₂ and the NO_x sink to HNO₃, which implies an OH increase, mostly in the upper troposphere (see Fig. ??). In addition, OH formation from NO+HO₂ reaction is enhanced if the NO loss on O₃ is less efficient.

15

Table 6. Atmospheric lifetimes (years) calculated in the ULAQ-CCM (experiment (b) in Table 1), relative to three species that include an OH reaction sink (i.e., CH₄, HCFC-22, CH₃CCl₃). CH₄ is predicted with the FBC approach, the other two species with specified surface mixing ratios (unchanged between G4 and RCP4.5). First column shows year 2000 values (as an average over the 1996-2005 decade); second column shows a model mean value from the SPARC (2013) report on lifetimes. Subsequent columns show the calculated lifetime anomalies due to sulfate geoengineering (average 2030-2069). Inside the square brackets we highlight the physical and chemical effects driving the lifetime changes (see text).

	1996-2005	Model mean [SPARC (2013)]	2030-2069 G4-RCP4.5 [All effects]	2030-2069 G4-G4[sn2] [Temperature]	2030-2069 G4-G4[sn3] [Transport]	2030-2069 G4[sn1]-RCP4.5 [UV+NO ₂ +O ₃]
CH ₄	8.8	8.7 ± 1.4	+1.33	+0.31	-0.28	+1.30
HCFC-22	10.0	10.7 ± 1.6	+0.83	+0.42	-0.29	+0.70
CH ₃ CCl ₃	4.6	4.6 ± 0.6	+0.50	+0.10	-0.10	+0.50

The strengthening of the Brewer-Dobson circulation affects essentially the upper tropospheric amount of SO_4 , CH_4 , NO_y and O_3 . This results in a negative anomaly for geoengineering SO_4 and for CH_4 (due to the enhanced lower stratospheric tropical confinement: see Fig. 8 and Fig. 5c) and a positive anomaly for NO_y and O_3 (due to the enhanced strat-trop downward flux). The induced OH anomaly is negative from CH_4 (~~which is an OH a net HO_x source~~) and O_3 (which is an OH sink in the upper troposphere). On the other hand, it is positive from SO_4 and NO_y (due to the increasing NO_x amount their negative or positive anomaly will produce). This positive NO_x anomaly induced in the upper troposphere by the enhanced stratospheric circulation mostly regulates the net positive OH change in the ULAQ-CCM, with decreasing lifetimes (column five in Table 6).

~~G4-G4(sn2) anomalies of $\text{NO}+\text{NO}_2$ mixing ratios in the upper troposphere and lowermost stratosphere, from ULAQ-CCM (b) (time average 2040-2049) (ppbv). The contour line increment is 0.005 ppbv. The sensitivity case G4-sn2 keeps temperature fixed at RCP4.5 values in the chemistry module.~~

6 Conclusions

In the present work, we have described ~~the effect how~~ an injection of 5-8 Tg of SO_2 per year would ~~have on~~ modify the large scale transport and lifetime of CH_4 , using two climate-chemistry coupled models, ULAQ-CCM and GEOSCCM, ~~both using~~. Both models use prescribed SST coming from two atmospheric-ocean coupled models: ~~CCSM-CAM4 and CESM, respectively for ULAQ-CCM and CESM for GEOSCCM~~. The model evaluation has shown that both models correctly simulate the vertical profiles for the chemical species under analysis (N_2O as a ~~passive quasi-passive~~ tracer and CH_4), the mean age of air and the vertical velocity w^* . Furthermore, the latitudinal heat fluxes have been ~~validated against compared with~~ ERA40 reanalysis in order to ~~validate evaluate~~ the skill of the models in correctly simulating the meridional transport.

We have shown that changes in the BDC due to lower stratospheric ~~warming aerosol heating~~ reduce the amount of CH_4 in the extra-tropical UTLS. ~~This is~~ both because of the strengthening of the downward branches of the BDC which brings more stratospheric air (poorer in CH_4) down in the upper troposphere and because of a greater isolation of the tropical pipe that reduces the amount of horizontal mixing. However, in order to properly assess the magnitude of the ~~variations of the transport transport perturbation~~ (whether it's horizontal mixing ~~of or~~ vertical fluxes), the addition of the feedback of the ocean has proven crucial. Cooler oceans allow for a further atmospheric stabilization of the atmosphere, and the cooling of the sub-Arctic regions produces important hemispheric asymmetries that are not found in fixed SSTs simulations. This points to a important limitation of pure CCM studies, with prescribed time-dependent SSTs consistent with a given RCP scenario. The large-scale transport effects of sulfate geoengineering on trace species can only be captured on all their non-linear aspects using coupled AOGCM simulations, which may quantify the SG induced changes on SSTs. These can, in turn, be used as input for the aerosol-chemistry-radiation-dynamics fully interactive CCM experiments.

Furthermore, we have shown that the changes in CH_4 lifetime and concentration take place because of a reduction of atmospheric OH, mostly due to three overlapping factors: (1) reduction in tropospheric water vapor caused by the surface cooling; (2) decrease in $\text{O}(^1\text{D})$ caused by a decrease in tropical tropospheric UV (~~since because~~ part of the incoming solar radiation

is scattered by the stratospheric aerosols, which also deplete ~~ozone~~stratospheric ozone); (3) ~~and a~~ decrease in NO_x production caused by the enhancing of heterogeneous chemistry (see visual summary in Fig. 14). Changes in stratospheric large-scale transport and strat-trop exchange may also contribute to perturb the tropospheric amount of OH, with a net effect whose sign results from simultaneous changes of CH_4 , NO_y , O_3 , SO_4 . All of these effects may cause ~~an increase of over a~~ CH_4 lifetime
20 increase of more than 1 year ~~for CH_4 lifetime~~ in the central decades of the experiment, leading, in turn, to an increase in methane mixing ratio of over 200 ppbv.

Overall, these changes produce in our radiative transfer model calculations a positive radiative forcing of more than $+0.1 \text{ W/m}^2$:
~~While this result goes in the opposite direction with respect to the desired effect of sulfate geoengineering,~~ a result that it's still one order of magnitude smaller than the direct negative radiative forcing of the aerosols, which has been estimated to be
25 ~~-1.4~~ $-1.2 \pm 0.5 \text{ W/m}^2$ for a 5 Tg SO_2/yr injection, considering simulations from a vast array of models (Visioni et al. (2017)).

In addition, gas species concentration changes (especially ozone) would also affect air quality and surface UV concentrations, which might have implications on human health, as already noted in Xia et al. (2017) and Nowack et al. (2016). As discussed in the present study, as well as in Nowack et al. (2016), Tilmes et al. (2012) and Pitari et al. (2014), the stratospheric ozone depletion induced by geoengineering solar radiation management techniques directly impact the tropospheric UV budget. The health impact of a surface UV enhancement (located only at mid-high latitudes in the case of sulfate geoengineering) may be
5 partly counterbalanced by the decreased tropospheric OH concentration and O_3 production.

Our analysis is limited to an atmospheric perturbation produced by sulfate geoengineering on photochemistry and large-scale transport: other important changes that would happen under this hypothetical scenario are the ones in natural surface emissions of CH_4 that would occur following changes in surface temperatures. Natural emissions would be reduced under sulfate geoengineering for three main reasons: (1) a reduction in surface temperatures that would in turn be connected with a highly probable reduction in rainfall, compared with the predicted increase under most future warming scenario (Trenberth (1998); Pandey et al. (2017)); this would reduce the amount of CH_4 produced by wetland areas, thus affecting the atmospheric methane concentration; (2) the increased surface deposition of sulfate under SG conditions would itself produce changes in emissions
5 from wetlands (Gauci et al. (2008)); (3) SG could help avert one of the possible risks of global warming, that is the emission of methane from permafrost thawing (Kohnert et al. (2017)). It remains to be investigated how much these effects, together, could offset the photochemical CH_4 increase resulting from our study.

Effects of sulfate geoengineering on CH₄ [photochemistry + transport]

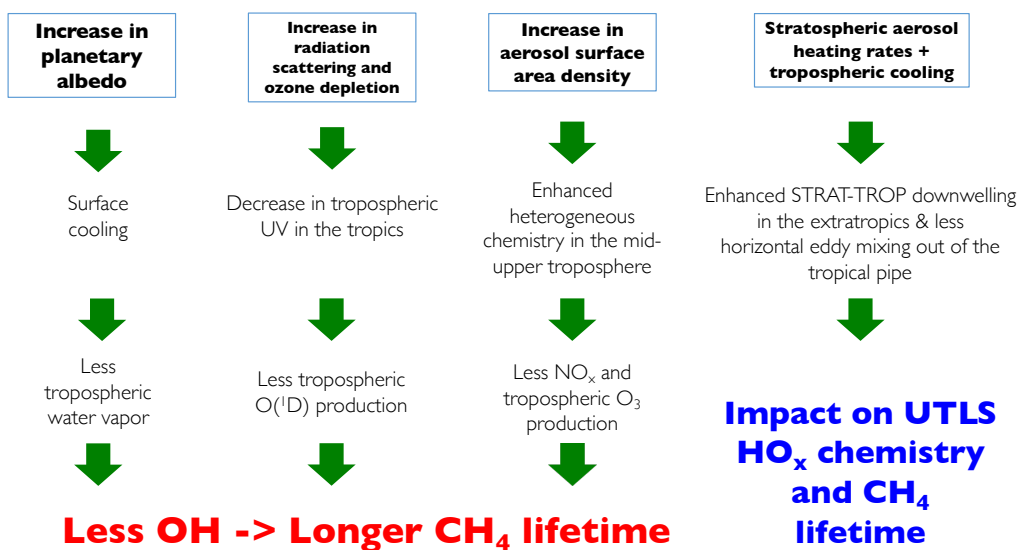


Figure 14. Visual representation of ~~all contributing factors to the changes that might occur~~ photochemical and transport effects of sulfate geoengineering on CH₄, as studied in ~~a SG scenario~~ this paper. Effects connected to perturbed CH₄ emissions due to surface cooling are not shown because they were not explicitly considered in this study. These effects are essentially: reductions in rainfall and halting of permafrost thawing.

Data availability. Data from model simulations are available from the corresponding author.

Competing interests. The authors declare no conflict of interest

- 10 *Acknowledgements.* Figure 1, ~~??, ?? and ??~~ S1, S2 and S3 were produced with the ESMValTool (Eyring et al. (2016)). GEOSCCM simulations performed by V. A. were supported by the NASA High-End Computing (HEC) Program through the NASA Center for Climate Simulations (NCCS) at Goddard Space Flight Center. I.C. acknowledges funding received from the European Union's Horizon 2020 research and innovation programme under grant agreement no. 641816 (CRESCENDO). The authors would like to thank R. de Richter and P.J. Nowack for their insightful comments regarding the conclusions of this study.

15

References

- Andrews, A. E., Boering, K. A., Daube, B. C., Wofsy, S. C., Loewenstein, M., Jost, H., Podolske, J. R., Webster, C. R., Herman, R. L., Scott, D. C., Flesch, G. J., Moyer, E. J., Elkins, J. W., Dutton, G. S., Hurst, D. F., Moore, F. L., Ray, E. A., Romashkin, P. A., and Strahan, S. E.: Mean ages of stratospheric air derived from in situ observations of CO₂, CH₄, and N₂O, *Journal of Geophysical Research: Atmospheres*, 20 106, 32 295–32 314, doi:10.1029/2001JD000465, <http://dx.doi.org/10.1029/2001JD000465>, 2001.
- Aquila, V., Oman, L. D., Stolarski, R., Douglass, A. R., and Newman, P. A.: The Response of Ozone and Nitrogen Dioxide to the Eruption of Mt. Pinatubo at Southern and Northern Midlatitudes, *Journal of the Atmospheric Sciences*, 70, 894–900, doi:10.1175/JAS-D-12-0143.1, <http://dx.doi.org/10.1175/JAS-D-12-0143.1>, 2013.
- Aquila, V., Garfinkel, C., Newman, P., Oman, L., and Waugh, D.: Modifications of the quasi-biennial oscillation by a geoengineering perturbation of the stratospheric aerosol layer, *Geophysical Research Letters*, 41, 1738–1744, 2014.
- Austin, J., Shindell, D., Beagley, S. R., Brühl, C., Dameris, M., Manzini, E., Nagashima, T., Newman, P., Pawson, S., Pitari, G., Rozanov, E., Schnadt, C., and Shepherd, T. G.: Uncertainties and assessments of chemistry-climate models of the stratosphere, *Atmospheric Chemistry and Physics*, 3, 1–27, doi:10.5194/acp-3-1-2003, <http://www.atmos-chem-phys.net/3/1/2003/>, 2003.
- Bais, A. F., Tourpali, K., Kazantzidis, A., Akiyoshi, H., Bekki, S., Braesicke, P., Chipperfield, M. P., Dameris, M., Eyring, V., Garny, H., Iachetti, D., Jockel, P., Kubin, A., Langematz, U., Mancini, E., Michou, M., Morgenstern, O., Nakamura, T., Newman, P. A., Pitari, G., Plummer, D. A., Rozanov, E., Shepherd, T. G., Shibata, K., Tian, W., and Yamashita, Y.: Projections of UV radiation changes in the 21st century: impact of ozone recovery and cloud effects, *Atmospheric Chemistry and Physics*, 11, 7533–7545, doi:10.5194/acp-11-7533-2011, <https://www.atmos-chem-phys.net/11/7533/2011/>, 2011.
- Banda, N., Krol, M., van Weele, M., van Noije, T., and Rockmann, T.: Analysis of global methane changes after the 1991 Pinatubo volcanic eruption, *Atmospheric Chemistry and Physics*, 13, 2267–2281, doi:10.5194/acp-13-2267-2013, <http://www.atmos-chem-phys.net/13/2267/2013/>, 2013.
- Banda, N., Krol, M., van Noije, T., van Weele, M., Williams, J. E., Sager, P. L., Niemeier, U., Thomason, L., and Rockmann, T.: The effect of stratospheric sulfur from Mount Pinatubo on tropospheric oxidizing capacity and methane, *Journal of Geophysical Research: Atmospheres*, 120, 1202–1220, doi:10.1002/2014JD022137, <http://dx.doi.org/10.1002/2014JD022137>, 2014JD022137, 2015.
- Bluth, G. J. S., Doiron, S. D., Schnetzler, C. C., Krueger, A. J., and Walter, L. S.: Global tracking of the SO₂ clouds from the June, 1991 Mount Pinatubo eruptions, *Geophysical Research Letters*, 19, 151–154, doi:10.1029/91GL02792, 1992.
- Canty, T., Mascioli, N. R., Smarte, M. D., and Salawitch, R. J.: An empirical model of global climate - Part 1: A critical evaluation of volcanic cooling, *Atmospheric Chemistry and Physics*, 13, 3997–4031, doi:10.5194/acp-13-3997-2013, <http://www.atmos-chem-phys.net/13/3997/2013/>, 2013.
- Crutzen, P. J.: Albedo Enhancement by Stratospheric Sulfur Injections: A Contribution to Resolve a Policy Dilemma?, *Climatic Change*, 77, 211–220, doi:10.1007/s10584-006-9101-y, <http://dx.doi.org/10.1007/s10584-006-9101-y>, 2006.
- Dlugokencky, E. J., Steele, L. P., Lang, P. M., and Masarie, K. A.: The growth rate and distribution of atmospheric methane, *Journal of Geophysical Research: Atmospheres*, 99, 17 021–17 043, doi:10.1029/94JD01245, <http://dx.doi.org/10.1029/94JD01245>, 1994.
- Engel, A., Mobius, T., Bonisch, H., Schmidt, U., Heinz, R., Levin, I., Atlas, E., Aoki, S., Nakazawa, T., Sugawara, S., Moore, F., Hurst, D., Elkins, J., Schauffler, S., Andrews, A., and Boering, K.: Age of stratospheric air unchanged within uncertainties over the past 30 years, *Nature Geosci*, 2, 28–31, <http://dx.doi.org/10.1038/ngeo388>, 2009.

- Eyring, V. and et al.: Overview of IGAC/SPARC Chemistry-Climate Model Initiative (CCMI) Community Simulations in Support of Upcoming Ozone and Climate Assessment, *SPARC Newsletter*, 40, 48–66, 2013.
- Eyring, V., Butchart, N., Waugh, D. W., Akiyoshi, H., Austin, J., Bekki, S., Bodeker, G. E., Boville, B. A., Bruhl, C., Chipperfield, M. P., Cordero, E., Dameris, M., Deushi, M., Fioletov, V. E., Frith, S. M., Garcia, R. R., Gettelman, A., Giorgetta, M. A., Grewe, V., Jourdain, L., Kinnison, D. E., Mancini, E., Manzini, E., Marchand, M., Marsh, D. R., Nagashima, T., Newman, P. A., Nielsen, J. E., Pawson, S., Pitari, G., Plummer, D. A., Rozanov, E., Schraner, M., Shepherd, T. G., Shibata, K., Stolarski, R. S., Struthers, H., Tian, W., and Yoshiki, M.: Assessment of temperature, trace species, and ozone in chemistry-climate model simulations of the recent past, *Journal of Geophysical Research: Atmospheres*, 111, n/a–n/a, doi:10.1029/2006JD007327, d22308, 2006.
- Eyring, V., Righi, M., Lauer, A., Evaldsson, M., Wenzel, S., Jones, C., Anav, A., Andrews, O., Cionni, I., Davin, E. L., Deser, C., Ehbrecht, C., Friedlingstein, P., Gleckler, P., Gottschaldt, K.-D., Hagemann, S., Juckes, M., Kindermann, S., Krasting, J., Kunert, D., Levine, R., Loew, A., Mäkelä, J., Martin, G., Mason, E., Phillips, A. S., Read, S., Rio, C., Roehrig, R., Senftleben, D., Sterl, A., van Ulft, L. H., Walton, J., Wang, S., and Williams, K. D.: ESMValTool (v1.0) – a community diagnostic and performance metrics tool for routine evaluation of Earth system models in CMIP, *Geoscientific Model Development*, 9, 1747–1802, doi:10.5194/gmd-9-1747-2016, <https://www.geosci-model-dev.net/9/1747/2016/>, 2016.
- Gauci, V., Dise, N. B., Howell, G., and Jenkins, M. E.: Suppression of rice methane emission by sulfate deposition in simulated acid rain, *Journal of Geophysical Research: Biogeosciences*, 113, n/a–n/a, doi:10.1029/2007JG000501, <http://dx.doi.org/10.1029/2007JG000501>, g00A07, 2008.
- Grooss, J. and Russell III, J. M.: Technical note: A stratospheric climatology for O₃, H₂O, CH₄, NO_x, HCl and HF derived from HALOE measurements, *Atmospheric Chemistry and Physics*, 5, 2797–2807, doi:10.5194/acp-5-2797-2005, <http://www.atmos-chem-phys.net/5/2797/2005/>, 2005.
- Hegglin, M. I., Gettelman, A., Hoor, P., Krichevsky, R., Manney, G. L., Pan, L. L., Son, S.-W., Stiller, G., Tilmes, S., Walker, K. A., Eyring, V., Shepherd, T. G., Waugh, D., Akiyoshi, H., Anel, J. A., Austin, J., Baumgaertner, A., Bekki, S., Braesicke, P., Bruhl, C., Butchart, N., Chipperfield, M. P., Dameris, M., Dhomse, S., Frith, S., Garny, H., Hardiman, S. C., Jockel, P., Kinnison, D. E., Lamarque, J. F., Mancini, E., Michou, M., Morgenstern, O., Nakamura, T., Olivie, D., Pawson, S., Pitari, G., Plummer, D. A., Pyle, J. A., Rozanov, E., Scinocca, J. F., Shibata, K., Smale, D., Teyssedre, H., Tian, W., and Yamashita, Y.: Multimodel assessment of the upper troposphere and lower stratosphere: Extra-tropics, *Journal of Geophysical Research: Atmospheres*, 115, D00M09, doi:10.1029/2010JD013884, <https://hal.archives-ouvertes.fr/hal-00510687>, 2010.
- IPCC: Climate Change 2013: The Physical Science Basis. Contribution of Working Group I to the Fifth Assessment Report of the Intergovernmental Panel on Climate Change, Cambridge Univ. Press, Cambridge, 2013.
- Kohnert, K., Serafimovich, A., Metzger, S., Hartmann, J., and Sachs, T.: Strong geologic methane emissions from discontinuous terrestrial permafrost in the Mackenzie Delta, Canada, *Scientific Reports*, 7, 5828, doi:10.1038/s41598-017-05783-2, <https://doi.org/10.1038/s41598-017-05783-2>, 2017.
- Kravitz, B., Robock, A., Boucher, O., Schmidt, H., Taylor, K. E., Stenchikov, G., and Schulz, M.: The Geoengineering Model Intercomparison Project (GeoMIP), *Atmospheric Science Letters*, 12, 162–167, doi:10.1002/asl.316, <http://dx.doi.org/10.1002/asl.316>, 2011.
- Kravitz, B., Robock, A., and Haywood, J. M.: Progress in climate model simulations of geoengineering, *Eos, Transactions American Geophysical Union*, 93, 340–340, doi:10.1029/2012EO350009, <http://dx.doi.org/10.1029/2012EO350009>, 2012.
- Labitzke, K. and McCormick, M. P.: Stratospheric temperature increases due to Pinatubo aerosols, *Geophysical Research Letters*, 19, 207–210, doi:10.1029/91GL02940, <http://dx.doi.org/10.1029/91GL02940>, 1992.

- Lamarque, J.-F., Bond, T. C., Eyring, V., Granier, C., Heil, A., Klimont, Z., Lee, D., Liousse, C., Mieville, A., Owen, B., Schultz, M. G., Shindell, D., Smith, S. J., Stehfest, E., Van Aardenne, J., Cooper, O. R., Kainuma, M., Mahowald, N., McConnell, J. R., Naik, V., Riahi, K., and van Vuuren, D. P.: Historical (1850-2000) gridded anthropogenic and biomass burning emissions of reactive gases and aerosols: methodology and application, *Atmospheric Chemistry and Physics*, 10, 7017–7039, doi:10.5194/acp-10-7017-2010, <http://www.atmos-chem-phys.net/10/7017/2010/>, 2010.
- Lambert, A., Grainger, R. G., Remedios, J. J., Rodgers, C. D., Corney, M., and Taylor, F. W.: Measurements of the evolution of the Mt. Pinatubo aerosol cloud by ISAMS, *Geophysical Research Letters*, 20, 1287–1290, doi:10.1029/93GL00827, <http://dx.doi.org/10.1029/93GL00827>, 1993.
- Long, C. S. and Stowe, L. L.: using the NOAA/AVHRR to study stratospheric aerosol optical thicknesses following the Mt. Pinatubo Eruption, *Geophysical Research Letters*, 21, 2215–2218, doi:10.1029/94GL01322, <http://dx.doi.org/10.1029/94GL01322>, 1994.
- McCormick, M. P. and Veiga, R. E.: SAGE II measurements of early Pinatubo aerosols, *Geophysical Research Letters*, 19, 155–158, doi:10.1029/91GL02790, <http://dx.doi.org/10.1029/91GL02790>, 1992.
- Morgenstern, O., Giorgetta, M. A., Shibata, K., Eyring, V., Waugh, D. W., Shepherd, T. G., Akiyoshi, H., Austin, J., Baumgaertner, A. J. G., Bekki, S., Braesicke, P., Bruhl, C., Chipperfield, M. P., Cugnet, D., Dameris, M., Dhomse, S., Frith, S. M., Garny, H., Gettelman, A., Hardiman, S. C., Hegglin, M. I., Jockel, P., Kinnison, D. E., Lamarque, J.-F., Mancini, E., Manzini, E., Marchand, M., Michou, M., Nakamura, T., Nielsen, J. E., Olivie, D., Pitari, G., Plummer, D. A., Rozanov, E., Scinocca, J. F., Smale, D., Teyssedre, H., Toohey, M., Tian, W., and Yamashita, Y.: Review of the formulation of present-generation stratospheric chemistry-climate models and associated external forcings, *Journal of Geophysical Research: Atmospheres*, 115, n/a–n/a, doi:10.1029/2009JD013728, <http://dx.doi.org/10.1029/2009JD013728>, d00M02, 2010.
- 35 Morgenstern, O., Hegglin, M. I., Rozanov, E., O'Connor, F. M., Abraham, N. L., Akiyoshi, H., Archibald, A. T., Bekki, S., Butchart, N., Chipperfield, M. P., Deushi, M., Dhomse, S. S., Garcia, R. R., Hardiman, S. C., Horowitz, L. W., Jockel, P., Josse, B., Kinnison, D., Lin, M., Mancini, E., Manyin, M. E., Marchand, M., Marecal, V., Michou, M., Oman, L. D., Pitari, G., Plummer, D. A., Revell, L. E., Saint-Martin, D., Schofield, R., Stenke, A., Stone, K., Sudo, K., Tanaka, T. Y., Tilmes, S., Yamashita, Y., Yoshida, K., and Zeng, G.: Review of the global models used within phase 1 of the Chemistry–Climate Model Initiative (CCMI), *Geoscientific Model Development*, 10, 639–671, doi:10.5194/gmd-10-639-2017, <https://www.geosci-model-dev.net/10/639/2017/>, 2017.
- Myhre, G., Shine, K., Radel, G., Gauss, M., Isaksen, I., Tang, Q., Prather, M., Williams, J., van Velthoven, P., Dessens, O., Koffi, B., Szopa, S., Hoor, P., Grewe, V., Borken-Kleefeld, J., Berntsen, T., and Fuglestedt, J.: Radiative forcing due to changes in ozone and methane caused by the transport sector, *Atmospheric Environment*, 45, 387 – 394, doi:<https://doi.org/10.1016/j.atmosenv.2010.10.001>, <http://www.sciencedirect.com/science/article/pii/S1352231010008629>, 2011.
- 5 Neu, J. L. and Plumb, R. A.: Age of air in a 'leaky pipe' model of stratospheric transport, *Journal of Geophysical Research: Atmospheres*, 104, 19 243–19 255, doi:10.1029/1999JD900251, <http://dx.doi.org/10.1029/1999JD900251>, 1999.
- Nowack, P. J., Abraham, N. L., Braesicke, P., and Pyle, J. A.: Stratospheric ozone changes under solar geoengineering: implications for UV exposure and air quality, *Atmospheric Chemistry and Physics*, 16, 4191–4203, doi:10.5194/acp-16-4191-2016, <https://www.atmos-chem-phys.net/16/4191/2016/>, 2016.
- 10 Pandey, S., Houweling, S., Krol, M., Aben, I., Monteil, G., Nechita-Banda, N., Dlugokencky, E. J., Detmers, R., Hasekamp, O., Xu, X., Riley, W. J., Poulter, B., Zhang, Z., McDonald, K. C., White, J. W. C., Bousquet, P., and Röckmann, T.: Enhanced methane emissions from tropical wetlands during the 2011 La Niña, *Scientific Reports*, 7, 45 759, doi:10.1038/srep45759, <http://www.ncbi.nlm.nih.gov/pmc/articles/PMC5385533/>, 2017.
- 15

- Pitari, G., Aquila, V., Kravitz, B., Robock, A., Watanabe, S., Cionni, I., Luca, N. D., Genova, G. D., Mancini, E., and Tilmes, S.: Stratospheric ozone response to sulfate geoengineering: Results from the Geoengineering Model Intercomparison Project (GeoMIP), *Journal of Geophysical Research: Atmospheres*, 119, 2629–2653, doi:10.1002/2013JD020566, <http://dx.doi.org/10.1002/2013JD020566>, 2014.
- 20 Pitari, G., Cionni, I., Di Genova, G., Sovde, O. A., and Lim, L.: Radiative forcing from aircraft emissions of NO_x: model calculations with CH₄ surface flux boundary condition, *Meteorologische Zeitschrift*, doi:10.1127/metz/2016/0776, <http://dx.doi.org/10.1127/metz/2016/0776>, 2016a.
- Pitari, G., Cionni, I., Di Genova, G., Visioni, D., Gandolfi, I., and Mancini, E.: Impact of Stratospheric Volcanic Aerosols on Age-of-Air and Transport of Long-Lived Species, *Atmosphere*, 7, <http://www.mdpi.com/2073-4433/7/11/149>, 2016b.
- Pitari, G., Di Genova, G., Mancini, E., Visioni, D., Gandolfi, I., and Cionni, I.: Stratospheric Aerosols from Major Volcanic Eruptions: A
25 Composition-Climate Model Study of the Aerosol Cloud Dispersal and e-folding Time, *Atmosphere*, 7, 75, doi:10.3390/atmos7060075, <http://dx.doi.org/10.3390/atmos7060075>, 2016c.
- Randles, C. A., Kinne, S., Myhre, G., Schulz, M., Stier, P., Fischer, J., Doppler, L., Highwood, E., Ryder, C., Harris, B., Huttunen, J., Ma, Y., Pinker, R. T., Mayer, B., Neubauer, D., Hittenberger, R., Oreopoulos, L., Lee, D., Pitari, G., Di Genova, G., Quaas, J., Rose, F. G., Kato, S., Rumbold, S. T., Vardavas, I., Hatzianastassiou, N., Matsoukas, C., Yu, H., Zhang, F., Zhang, H., and Lu, P.: Intercomparison of
30 shortwave radiative transfer schemes in global aerosol modeling: results from the AeroCom Radiative Transfer Experiment, *Atmospheric Chemistry and Physics*, 13, 2347–2379, doi:10.5194/acp-13-2347-2013, <https://www.atmos-chem-phys.net/13/2347/2013/>, 2013.
- Robock, A., Kravitz, B., and Boucher, O.: Standardizing experiments in geoengineering, *Eos, Transactions American Geophysical Union*, 92, 197–197, doi:10.1029/2011EO230008, <http://dx.doi.org/10.1029/2011EO230008>, 2011.
- Russell, J. M., Gordley, L. L., Park, J. H., Drayson, S. R., Hesketh, W. D., Cicerone, R. J., Tuck, A. F., Frederick, J. E., Harries,
35 J. E., and Crutzen, P. J.: The Halogen Occultation Experiment, *Journal of Geophysical Research: Atmospheres*, 98, 10 777–10 797, doi:10.1029/93JD00799, <http://dx.doi.org/10.1029/93JD00799>, 1993.
- Sankey, D. and Shepherd, T. G.: Correlations of long-lived chemical species in a middle atmosphere general circulation model, *Journal of Geophysical Research: Atmospheres*, 108, n/a–n/a, doi:10.1029/2002JD002799, <http://dx.doi.org/10.1029/2002JD002799>, 4494, 2003.
- Schauffler, S. M. and Daniel, J. S.: On the effects of stratospheric circulation changes on trace gas trends, *Journal of Geophysical Research: Atmospheres*, 99, 25 747–25 754, doi:10.1029/94JD02223, <http://dx.doi.org/10.1029/94JD02223>, 1994.
- Soden, B. J., Wetherald, R. T., Stenchikov, G. L., and Robock, A.: Global Cooling After the Eruption of Mount Pinatubo: A Test of Climate
5 Feedback by Water Vapor, *Science*, 296, 727–730, doi:10.1126/science.296.5568.727, <http://science.sciencemag.org/content/296/5568/727>, 2002.
- SPARC: Chapter 5: Model Estimates of Lifetimes in SPARC Report on Lifetimes of Stratospheric Ozone-Depleting Substances, Their Replacements, and Related Species. Chipperfield, M. and Q. Liang, et al. , Tech. rep., SPARC, <http://www.sparc-climate.org/publications/sparc-reports/>, 2013.
- SPARC-CCMVal(2010): SPARC Report on the evaluation of chemistry-climate models, SPARC Report, WCRP-132, WMO/TD-No, 2010.
- 10 Spivakovsky, C. M., Logan, J. A., Montzka, S. A., Balkanski, Y. J., Foreman-Fowler, M., Jones, D. B. A., Horowitz, L. W., Fusco, A. C., Brenninkmeijer, C. A. M., Prather, M. J., Wofsy, S. C., and McElroy, M. B.: Three-dimensional climatological distribution of tropospheric OH: Update and evaluation, *Journal of Geophysical Research: Atmospheres*, 105, 8931–8980, doi:10.1029/1999JD901006, <http://dx.doi.org/10.1029/1999JD901006>, 2000.
- Strahan, S. E., Douglass, A. R., Stolarski, R. S., Akiyoshi, H., Bekki, S., Braesicke, P., Butchart, N., Chipperfield, M. P., Cugnet, D., Dhomse,
15 S., Frith, S. M., Gettelman, A., Hardiman, S. C., Kinnison, D. E., Lamarque, J.-F., Mancini, E., Marchand, M., Michou, M., Morgenstern,

- O., Nakamura, T., Olivie, D., Pawson, S., Pitari, G., Plummer, D. A., Pyle, J. A., Scinocca, J. F., Shepherd, T. G., Shibata, K., Smale, D., Teysse, H., Tian, W., and Yamashita, Y.: Using transport diagnostics to understand chemistry climate model ozone simulations, *Journal of Geophysical Research: Atmospheres*, 116, n/a–n/a, doi:10.1029/2010JD015360, <http://dx.doi.org/10.1029/2010JD015360>, d17302, 2011.
- 20 Taylor, K. E., Stouffer, R. J., and Meehl, G. A.: An overview of CMIP5 and the experiment design, *Bulletin of the American Meteorological Society*, 93, 485, 2012.
- Tilmes, S., Garcia, R. R., Kinnison, D. E., Gettelman, A., and Rasch, P. J.: Impact of geoengineered aerosols on the troposphere and stratosphere, *Journal of Geophysical Research: Atmospheres*, 114, doi:10.1029/2008JD011420, <http://dx.doi.org/10.1029/2008JD011420>, d12305, 2009.
- 25 Tilmes, S., Kinnison, D. E., Garcia, R. R., Salawitch, R., Canty, T., Lee-Taylor, J., Madronich, S., and Chance, K.: Impact of very short-lived halogens on stratospheric ozone abundance and UV radiation in a geo-engineered atmosphere, *Atmospheric Chemistry and Physics*, 12, 10945–10955, doi:10.5194/acp-12-10945-2012, <http://www.atmos-chem-phys.net/12/10945/2012/>, 2012.
- Tilmes, S., Lamarque, J.-F., Emmons, L. K., Kinnison, D. E., Marsh, D., Garcia, R. R., Smith, A. K., Neely, R. R., Conley, A., Vitt, F., Val Martin, M., Tanimoto, H., Simpson, I., Blake, D. R., and Blake, N.: Representation of the Community Earth System Model (CESM1) CAM4-chem within the Chemistry-Climate Model Initiative (CCMI), *Geoscientific Model Development*, 9, 1853–1890, doi:10.5194/gmd-9-1853-2016, <http://www.geosci-model-dev.net/9/1853/2016/>, 2016.
- 30 Trenberth, K. E.: Atmospheric Moisture Residence Times and Cycling: Implications for Rainfall Rates and Climate Change, *Climatic Change*, 39, 667–694, doi:10.1023/A:1005319109110, <https://doi.org/10.1023/A:1005319109110>, 1998.
- Trepte, C. R. and Hitchman, M. H.: Tropical stratospheric circulation deduced from satellite aerosol data, *Nature*, 355, 626–628, doi:10.1038/355626a0, 1992.
- Urban, J., Pommier, M., Murtagh, D. P., Santee, M. L., and Orsolini, Y. J.: Nitric acid in the stratosphere based on Odin observations from 2001 to 2009 ? Part 1: A global climatology, *Atmospheric Chemistry and Physics*, 9, 7031–7044, doi:10.5194/acp-9-7031-2009, <http://www.atmos-chem-phys.net/9/7031/2009/>, 2009.
- 675 Visioni, D., Pitari, G., and Aquila, V.: Sulfate geoengineering: a review of the factors controlling the needed injection of sulfur dioxide, *Atmos. Chem. Phys.*, 17, 3879–3889, doi:10.5194/acp-17-3879-2017, <http://www.atmos-chem-phys.net/17/3879/2017/>, 2017.
- Wecht, K. J., Jacob, D. J., Frankenberg, C., Jiang, Z., and Blake, D. R.: Mapping of North American methane emissions with high spatial resolution by inversion of SCIAMACHY satellite data, *Journal of Geophysical Research: Atmospheres*, 119, 7741–7756, doi:10.1002/2014JD021551, <http://dx.doi.org/10.1002/2014JD021551>, 2014JD021551, 2014.
- 680 Worden, J., Kulawik, S., Frankenberg, C., Payne, V., Bowman, K., Cady-Peirara, K., Wecht, K., Lee, J.-E., and Noone, D.: Profiles of CH₄, HDO, H₂O, and N₂O with improved lower tropospheric vertical resolution from Aura TES radiances, *Atmospheric Measurement Techniques*, 5, 397–411, doi:10.5194/amt-5-397-2012, <http://www.atmos-meas-tech.net/5/397/2012/>, 2012.
- 685 Xia, L., Nowack, P. J., Tilmes, S., and Robock, A.: Impacts of Stratospheric Sulfate Geoengineering on Tropospheric Ozone, *Atmospheric Chemistry and Physics Discussions*, 2017, 1–38, doi:10.5194/acp-2017-434, <http://www.atmos-chem-phys-discuss.net/acp-2017-434/>, 2017.